Development of high performance moisture barrier coating for PET bottles

Chiara Ascione

Abstract

Development of high performance moisture barrier coating for PET bottles.

Chiara Ascione

Polyethylene Terephthalate (PET) is one of the most common polymers for packaging applications, because of its properties and versatility. The limit of the use of PET containers in packaging is its low barrier to gases, with a negative impact on the quality of the product. The project intends to improve water vapor barrier properties of PET commercial containers. Possible technological routes should be amenable to an industrial implementation, sustainable and with no impact on bottle appearance. Coating technology can satisfy all the requirements for the industrial implementation, because high performances can be achieved adding a thin barrier material, minimizing the negative impact on the recycling process.

The concept at the basis of the PhD activity is the realization of a coating based on a PET compatible polymer, eventually loaded with impermeable 2D-additives, to apply by spray coating on PET bottles. The design of the coating matrix starts from prevalently amorphous vinyl alcohol polymer (HAVOH), that is a high oxygen barrier polymer. HAVOH is a water-soluble polymer, hence a chemical crosslinking agent is required to achieve the insolubility of the coating for water. Crosslinker concentration and crosslinking conditions are investigated by solubility test. ▆▆▆▆▆▆▆▆▆▆▆▆▆▆▆▆▆▆▆▆▆▆▆▆▆▆▆▆▆▆▆▆ WVTR tests on cross-linked HAVOH coating (35µm thickness) show undetectable WVTR (<0.005 g m-2 day-1), even at high relative humidity percentage. Coatings formula designed can be easy removed from PET washing with caustic solution (1%wt) at 85ºC, according to recycling test protocol.

Graphene-based additives (graphene, graphene oxide, reduced graphene oxide) are considered as possible additives for the developed coating, to obtain undetectable WVTR, even with thinner coating. Graphene-based fillers are widely used in literature to improve gas barrier properties of a polymer matrix. They reduce gas solubility, due to insolubility of gas in the nanosheets, and diffusivity, as the gas molecules must move around the impermeable nanosheets to diffuse through the polymer. Compared to graphene and GO, RGO is the potential additive for this application.

Developed coating is deposited on real PET bottles, to evaluate optimal spray coating conditions, such as air and liquid flow rate, and drying rate. To increase the wettability of the coating solution on PET, the possibility of combine coating with anti-static solvent is considered.

Contents

*"God made the bulk;
the surface was invented by the devil."*

Wolfgang Pauli

CHAPTER
1

Introduction

In this chapter, the aim of the PhD project is discussed, presenting the scientific and industrial problematics at the basis of the work and the main objectives of the activity (§1.1). Then, the organization of the thesis is briefly illustrated (§ 1.2).

1.1
PhD Aim

Nowadays, polymeric materials are widely used in packaging, replacing conventional materials (metals, ceramics and paper). The benefits achieved using polymers in packaging application are attributable to their unique characteristics. For example, properties easy to find in a polymeric material, such as transparency and lightweight, influence positively the final product appearance. Other properties, such as low cost and ease of processing, give advantages in the realization of the final product. However, the handicap of the use polymers in packaging, compared to conventional materials, is their inherent permeability to gases and vapors, including oxygen, carbon dioxide, and organic vapors. Polymers most frequently used in food packaging are polyethylene, polypropylene, polystyrene, polyvinyl chloride (PVC), and polyethylene terephthalate.

Polyethylene Terephthalate (PET) is becoming the packaging material of choice for many food products, especially beverages (carbonated drinks) and mineral waters, because of its properties and versatility. PET is a clear, flexible and a low-cost material with a good resistance to heat, mineral oils, solvents and acids. [Arora and Padua (2009)]. For these unique properties, nowadays PET bottles have gradually replaced glass and metal bottles as the most common packaging for liquid food and, especially for carbonated drinks [Shirakura et al. (2006)].
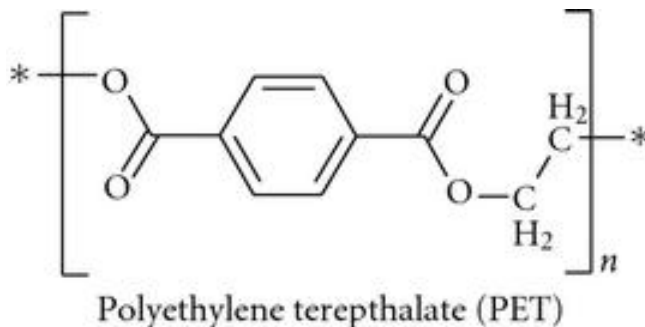
Figure 1.1 Chemical Formula of PET [Prasad et al. (2011)].

In 1976, PET bottles were first introduced in Japan for soy sauce. Since the first commercial debut in 1978 for the soft drink market in the U.S.A., the total amount of PET bottle usage has rapidly expanded to approximately 250 billion units in the year of 2004, corresponding to 10 million metric tons of PET resin, and a further growth by an average of over 10% annually is expected [Witte (2003)]. Compared to other general plastic materials, PET containers have good gas barrier properties, but not sufficient to preserve the product quality, due to the non-negligible permeation of gas molecules across the containers wall. In fact, for PET drink bottles, the permeation of O_2 from the air into the bottle accelerates the deterioration of the beverage, causing the loss of flavor and vitamins. Furthermore, in case of PET bottles containing carbonated soft drink, the release of CO_2 from the bottle affects the fizziness of the product [Berlinet et al. (2008)].

PET containers are mainly used for drink industry, but the new trend is their use in the detergents industry. The disadvantage is the low water vapor barrier of PET, because the permeation of water vapor from the bottle walls causes a decrease of the quantity of the product inside the container. In fact, in North America, Procter & Gamble needs to overfill PET bottles (used in all Sectors and a growing segment), for legal compliance, to guarantee a minimum shelf life (2 years). This is a very expensive operation, whereas a proper barrier PET bottle (without impacting end-of-life, e.g. recycling) could prevent this expense. Hence, providing an efficient and cost-effective procedure to develop a PET container with significantly improved moisture barrier represent a very interesting challenge.

The developed solution should be easy to implement at lowest cost, sustainable with no impact on recycling and on First Moment of Truth [Nelson and Ellison (2005)]. The techniques recently proposed in the technical and scientific literature to achieve high gas barrier for PET containers can be divided in four categories:

- *Barrier coatings*. Thin coatings [Deilmann et al. (2009)] or organic barrier coating [Compton et al. (2010)] can be applied inside or outside PET containers.
- *Multilayer Structures*. A structure of different alternated materials can be applied outside the container, by deposition-dry steps (e.g. layer by layer structures) [Yang et al. (2013)].
- *Nanocomposites*. Gas barrier nanofillers can be introduced in PET matrix. [Lange and Wyser (2003)]

- *Sleeves*. A shrinkable barrier sleeve can be applied outside PET containers [Su et al. (2014)].

The mentioned categories differ for level of technological maturity and suitability in an industrial packaging process. For example, the realization of multilayer structures results to be difficult to implement in a fast industry process because it is composed by several steps deposition-dry. Furthermore, layers of different materials could negatively influence the recyclability of PET bottles.

Compared to other categories, in the case of a remarkable improvement of barrier for PET containers, barrier coating approach is the most industrially feasible solution, in terms of container performance, economics and recyclability. In fact, the presence of a coating usually doesn't influence the recyclability of the container, and it is expected as the lowest cost operation. For these reasons, barrier coatings have the largest growth potential among the barrier enhancement technologies in packaging and coated PET containers are an expanding trend, especially in Japanese market [Nakaya et al. (2015)].

The aim of the PhD project was the development of a new high-performance moisture barrier coating for PET containers. the design of the moisture barrier coating was performed starting from the choice of a coating polymer to modify to achieve high moisture barrier effect. The choice was done considering the compatibility of the polymer with PET (wettability, adhesion), its industrial feasibility (ease of preparation of coating solution and spraying), and its influence on final packaging (transparency, roughness). The possibility of adding 2D-additives to coating to further improve the barrier effect was considered. In fact, the dispersion of 2D impermeable additives in a polymer matrix can increase its gas barrier properties due to the increase of tortuosity of the gas molecules path across the polymer matrix. The developing of the coating was performed considering at first PET films, before running it on real bottles. Lastly, the coating developed was applied on real PET bottles to establish optimal spray coating parameters.

1. 2
Thesis Organization

The present dissertation is divided into six chapters. *Chapters 2* and *3* provide principles of theory of permeability and the state of art of techniques used during the work. *Chapters 4*, *5*, and *6* provide the activity performed during the PhD. Each one of this last three chapters is basically self-consistent: at the beginning, a preliminary introduction to the central topic of the section is provided together with a brief overview of the state-of-the-art, then the results of the investigations are presented and discussed. Lastly, future developments of the topic are discussed.

Chapter 2, named "*Permeability of Polymeric Packaging Materials*" provides the background of the theory of permeability applied to polymers, discussing concepts of permeability, solubility, diffusion, and transmission rate.

Chapter 3, named "*Techniques of Gas Barrier Coatings Deposition*", introduces the main techniques for the gas barrier coatings deposition. In particular, two techniques, spray coating and rod coating, employed in this work are discussed.

In *Chapter 4*, named "*Development of a Water Vapor Barrier Coating Matrix*", the design of the water vapor barrier coating developed is discussed, starting from the choice of the polymer to modify. Then, the polymer modifications and their effect on water vapor transmission rate are evaluated. Lastly, tests to evaluate the industrial feasibility of the developed coating are performed.

In *Chapter 5*, named "*Evaluation of 2D-additives*", the possibility to introduce additives in the developed coating is discussed. The effect of the addition of graphene-based additives on the water vapor transmission rate of the coating is evaluated.

Chapter 6, named "*Application of developed coating matrix on real PET bottles*", represent the passage from the lab-scale to the industrial process. In this chapter, developed coating matrix discussed in *Chapter 4* is applied on real PET bottles, and spray conditions are evaluated to obtain a high quality final product.

Finally, the *Conclusions* section is dedicated to a brief summing-up of the activities, aiming to highlight the main findings of the performed research.

In *Material & Characterization*, list of raw materials used is reported. Furthermore, instruments description and conditions of tests were reported.

CHAPTER

2

Permeability of Polymeric Packaging Materials

In this chapter, theory at the basis of permeability of polymeric packaging materials is illustrated. At first, concepts of permeability, diffusion, solubility and transmission rate are discussed in case of steady-state and unsteady-state conditions (§2.1). Then, parameters that can affect permeability are presented, with particular attention to the dependence of permeability from temperature (§2.2). Lastly, permeability of multilayer structured materials is illustrated, that is the case in which a coating is applied on the packaging material (§2.3).

<div align="right">

2. 1
Theory of Permeability

</div>

Packaging materials based on polymers are permeable to varying degrees to small molecules, such as gases, water vapor and organics compounds, in contrast to packaging materials based on glass or metals. The barrier properties of plastics indicate their resistance to sorption and diffusion of these small molecules [Campbell-Platt (2017)]. Permeability and integrity of package can affect negatively product properties, due to a gas and vapor exchange between the product and the external environment.

Gases and vapors can pass through polymeric materials, by two processes: pore effect, and solubility-diffusion effect. In the first case, gases and vapors flow through microscopic pores, pinholes and cracks in the material. In the second case, gases and vapors dissolve in the polymer at one surface, diffuse through the polymer due to a concentration gradient and evaporate at the other surface of the polymer. This "solution-diffusion" process (also known as "activated diffusion") is described as true permeability. Most polymers exhibit both effects, especially when sufficiently thin [Robertson (2016)].

2.1.1 Steady-state conditions

Under steady-state conditions, a gas or vapor will diffuse through a polymer at a constant rate if a constant pressure difference is maintained across the polymer. The diffusive flux, J, of a permeant in a polymer can be defined as the amount passing through a plane (surface) of unit area normal to the direction of flow during unit time:

$$J = Q/(A \cdot t) \tag{2.1}$$

where Q is the total amount of gas or vapors (permeants) which pass through area A (packaging surface) during time t.

The rate of permeation and the concentration gradient are related by direct proportionality in Fick's first law:

$$J = -D \frac{\delta c}{\delta x} \tag{2.2}$$

where c is the concentration of the permeant, D is defined as the diffusion coefficient, and $\delta c / \delta x$ is the concentration gradient of the permeant across a thickness δx [Campbell-Platt (2017)].
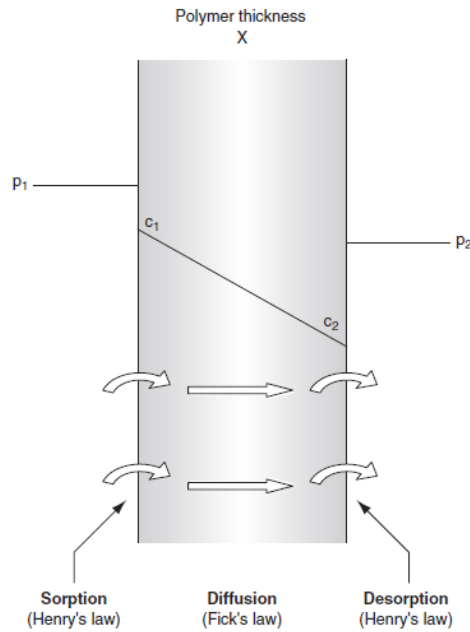
Figure 2.1 Permeability model for gas or vapor transfer through a polymer [Robertson (2016)].

The diffusion coefficient reflects the speed at which the permeant diffuses through the polymer. It is a function of temperature and may be a function of concentration. Equation (2.2) can be used to calculate the steady-state rate of diffusion, assuming that D is constant, and the concentration is a function only of the geometric position inside the polymer [Robertson (2016)].

In figure 2.1 is illustrated a polymeric material X mm thick of area A, exposed to a permeant at pressure p_1 on one side and at a lower pressure p_2 on the other. The concentration of permeant in the first layer of the polymer is c_1 and in the last layer c_2. When steady-state diffusion has been reached, J is constant and equation (2.2)

can be integrated across the total thickness of the polymer X, and between the two concentrations, assuming D to be constant and independent of c:

$$JX = -D(c_2 - c_1) \tag{2.3}$$

and

$$J = D \frac{(c_1 - c_2)}{x} \tag{2.4}$$

By substituting for J using equation (2.1), the quantity of permeant diffusing through a polymer of area A in time t can be calculated:

$$Q = D \frac{(c_1 - c_2)}{x} At \tag{2.5}$$

Rather than concentration, when the permeant is a gas, is more convenient to measure the vapor pressure p which is at equilibrium with the polymer [Zeman and Kubik (2007)]. At sufficiently low concentrations, Henry's law applies, and c can be expressed as:

$$c = Sp \tag{2.6}$$

where S is the solubility coefficient (Henry's constant) of the permeant in the polymer. S reflects the amount of permeant in the polymer. By combining equations (2.5) and (2.6):

$$Q = DS \frac{(p_1 - p_2)}{x} At \tag{2.7}$$

At thermodynamic equilibrium, the gas permeability coefficient P is given by:

$$P = DS \tag{2.8}$$

and is the product of a kinetic term (diffusivity D) which reflects the dynamics of the penetrant–polymer system and of a thermodynamic term (solubility S) which depends on the penetrant–polymer interactions. These quantities are functions of optional volume, cohesive energy and polymer morphology [McBride et al. (1979)]. Hence, permeability represents the ease with which a gas permeates through a polymer when subjected to a pressure gradient and can be written as:

$$P = \frac{Qx}{S(p_1 - p_2)t} \tag{2.9}$$

or

$$\frac{Q}{t} = \frac{P}{x} A \Delta p \tag{2.10}$$

The term P/X is called the *permeance* [Campbell-Platt (2017)]. The above treatment of steady-state diffusion assumes that both D and S are independent of concentration, but in practice deviations do occur. In fact, equation (2.9) does not hold when there is interaction such as occurs between hydrophilic materials, such as PVA or EVOH, and water vapor, or for heterogeneous materials such as coated or laminated films. The property is then defined as the *transmission rate* (TR) of the material, where:

$$TR = \frac{Q}{At} \tag{2.11}$$

where Q is the amount of permeant passing through the polymer, A is the area, t is the time.
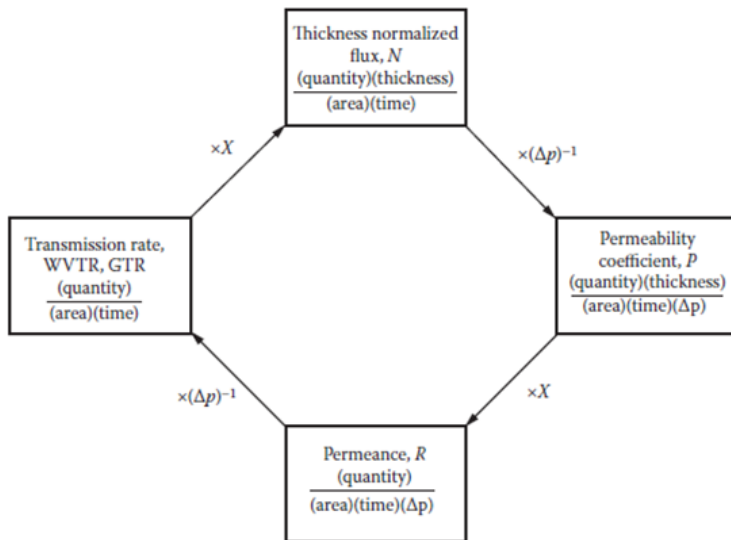
Figure 2.2 Relationship between transmission rate, TR, thickness normalized flux N, permeance R and permeability coefficient P [Hernandez (1997)].

Permeabilities of polymers to water and organic compounds are often presented in this way, and in the case of water and oxygen, the terms WVTR (water vapor

transmission rate) and OTR (oxygen transmission rate) are in common usage [Campbell-Platt (2017)]. Relationship between transmission rate, TR, thickness normalized flux N, permeance R and permeability coefficient P [Hernandez (1997)] is reported in figure 2.2.

2.1.2 Unsteady-state conditions

There is an interval before the steady-state is achieved, due to the finite diffusion rate of the solute in the polymer. The situation which exists during this transient period, where concentration varies with time, is described by Fick's second law:

$$\frac{\delta c}{\delta t} = D \frac{\delta^2 c}{\delta x^2} \tag{2.12}$$

which is a derivative of the first law. Solutions have been found for various boundary conditions; a useful solution in the present context is for the case of a finite solid with a concentration-independent diffusion constant, where the polymer is initially free from gas and one surface is then exposed to gas at pressure p_1 giving a concentration in the surface layer of c_1 [Robertson (2016)]. With these boundaries conditions:

$$Q = \frac{Dc_1}{x}\left(t - \frac{x^2}{6D}\right) = \frac{Dc_1 t}{x} - \frac{c_1 x}{6} \tag{2.13}$$

which Q is a linear function of t. Hence, the amount of gas permeating through the polymer increases linearly with time once the steady-state has been reached, as reported in figure 2.3.

If the linear portion of the steady-state line AB is extrapolated back to $Q = 0$ where the intercept $t = \tau$, then from equation (2.13):

$$\frac{Dc_1 \tau}{X} = \frac{c_1 X}{6} \tag{2.14}$$

or

$$D = \frac{X^2}{6\tau} \tag{2.15}$$

and

$$\tau = \frac{X^2}{6D} \tag{2.16}$$

The value τ is called the time lag and is the intercept on the time axis of the extrapolated steady-state portion of the curve in figure 2.2.
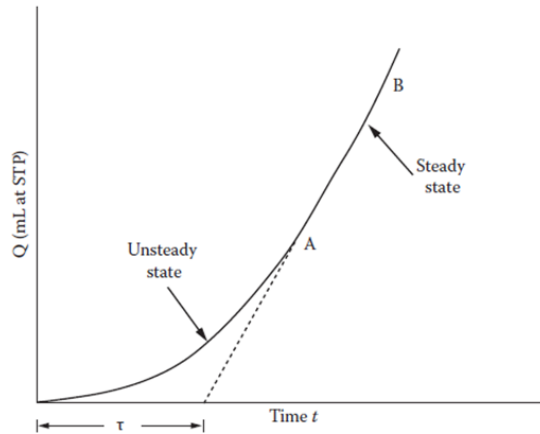
Figure 2.3 Typical permeation and time lag curve where Q is the amount of permeant that has permeated as a function of time t and τ is the time lag [Mathlouthi (2013)].

Thus, all three parameters of interest can be calculated from a single experiment. The permeability coefficient P is obtained by calculating the steady-state permeation rate Q/t (the slope of the asymptotic line in figure 2.3 and substituting in equation (2.7)). The diffusion coefficient D is obtained from the time lag τ, in the equation (2.13), and the solubility coefficient S is calculated as P/D. Under ordinary conditions for a constant D, the steady-state of flow is reached after a period amounting to about 2.7τ [Robertson (2016)].

2.2
Parameters affecting packaging permeability

Polymeric materials present a wide range of properties, depending on their chemical structure, method of preparation and processing conditions. Some of these properties can influence the polymer permeability [Zeman and Kubik (2007)]. Permeability is influenced both from the chemical structure of the polymer and the permeant, that determine the level of interaction. There is a value of permeability for each pair of polymer/permeant [Ashley (1985)]. For example, in case of hydrophilic polymers, humidity can increase the permeability, due to the interaction between water molecules and hydrophilic groups on polymer chains.

Polymer morphology also influences permeability: an increase in polymer crystallinity (density), orientation, or crosslinking, usually decreases permeability [Valentas et al. (1997)].

Temperature influences both polymer solubility and diffusivity. The temperature dependence of the solubility coefficient over relatively small ranges of temperature can be represented by an Arrhenius-type relationship:

$$S = S_0 \exp(-\Delta H_s / RT) \tag{2.17}$$

where ΔH_s is the heat of sorption. For the permanent gases, ΔH_s is small and positive and therefore S increases slightly with temperature. For easily condensable vapors, ΔH_s is negative due to the contribution of the heat of condensation, and thus S decreases with increasing temperature [Robertson (2016)].

The temperature dependence of the diffusion coefficient can also be represented by an Arrhenius-type relationship:

$$D = D_0 \exp(-E_d / RT) \tag{2.18}$$

where E_d is the activation energy for the diffusion process. E_d is always positive and D increases with increasing temperature. From equations (2.17) (2.18), it follows that

$$P = P_0 \exp(-E_p / RT) = D_0 S_0 \exp[-(E_p + \Delta H_s) / RT)] \tag{2.19}$$

where E_p (=E_d + ΔH_s) is the apparent activation energy for permeation.

Hence, it follows that the permeability coefficient of a specific polymer-permeant system may increase or decrease with increases in temperature depending on the relative effect of temperature on the solubility and diffusion coefficients of the system. Generally, the solubility coefficient increases with increasing temperature for gases and decreases for vapors, and the diffusion coefficient increases with temperature for both gases and vapors. For these reasons, permeability coefficients of different polymers determined at one temperature may not be in the same relative order at other temperatures [Campbell-Platt (2017)].

2.3

Permeability of multilayers packaging materials

Many products require more protection than a single material to give the product its intended shelf life. Where increased barriers to gases and/or moisture vapor are necessary, it is more economical to incorporate a thin layer of barrier material than to simply increase the thickness of a monolayer [Robertson (2016)].
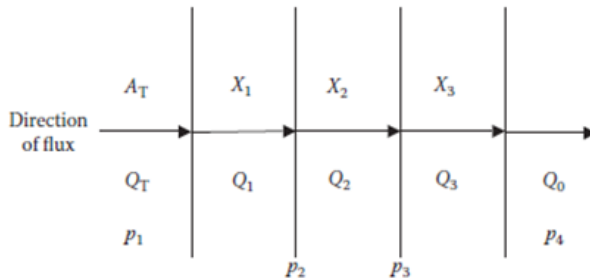
Figure 2.4 Schematic representation of permeation through three materials in series [Robertson (2016)].

Multilayer materials can be considered as several membranes in series. In the case of three layers, as schematically reported in figure 2.4, the total thickness is the sum of single layers thickness:

$$X_T = X_1 + X_2 + X_3 \qquad (2.20)$$

Assuming steady-state flux, the rate of permeation through each layer must be constant:

$$Q_T = Q_1 + Q_2 + Q_3 = Q_0 \qquad (2.21)$$

The areas will also be constant:

$$A_T = A_1 + A_2 + A_3 \qquad (2.22)$$

From the equation (2.10), is possible to calculate that:

$$\frac{Q_T}{t} = \frac{P_1}{X_1} A_1 (p_1 - p_2) = \frac{P_2}{X_2} A_2 (p_2 - p_3) = \frac{P_1}{X_1} A_3 (p_3 - p_4) \qquad (2.23)$$

By rearranging equation 2.23 and writing it for the case of permeation through the multilayer:

$$\frac{Q_T X_T}{t A_T P_T} = (p_1 - p_4) = \Delta p_i \qquad (2.24)$$

now, because:

$$(p_1 - p_4) = (p_1 - p_2) + (p_2 - p_3) + (p_3 - p_4) \qquad (2.25)$$

therefore:

$$\frac{Q_T X_T}{t A_T P_T} = \frac{Q_T}{t A_T} \left[\frac{X_1}{P_1} + \frac{X_2}{P_2} + \frac{X_3}{P_3} \right] \qquad (2.26)$$

and:

$$\frac{X_T}{P_T} = \frac{X_1}{P_1} + \frac{X_2}{P_2} + \frac{X_3}{P_3} \qquad (2.27)$$

or:

$$P_T = \frac{X_T}{\left(\frac{X_1}{P_1}\right) + \left(\frac{X_2}{P_2}\right) + \left(\frac{X_3}{P_3}\right)} \qquad (2.28)$$

Thus, if the individual thicknesses and permeability coefficients are known for each layer and provided that the permeability coefficients are independent of pressure, the equation (2.28) can be used to calculate the permeability coefficient for any multilayer material. If they are not independent of pressure, then differing permeability coefficients will be obtained depending on the positioning of the layers [Robertson (2016)].

CHAPTER

3

Techniques of Gas Barrier Coatings Deposition

In this chapter, a brief description of main barrier coating and thin films deposition techniques is presented. At first, the most advanced and high-cost technology is discussed: Chemical Vapor Deposition and, in details, Plasma Enhanced Chemical Vapor Deposition (§ 3.1). Then, the most industrially feasible and low-cost techniques are illustrated: Wire-Wound Rod Coating (§ 3.2) and Spray Coating, focusing on High Volume Low Pressure Spray Coating (§ 3.3).

3.1

Chemical Vapor Deposition

Chemical vapor deposition (CVD) is a process used to deposit or grow thin films, crystalline or amorphous, from solid, liquid or gaseous precursors of many materials [Ferrari et al. (2014)]. A trend of expanding its applications from initial mass semiconductor and microelectronics production to a wide range of applications has gained momentum in recent years, because of intensive research and development work being undertaken by academic and industrial researchers [Yan and Xu (2010)].

CVD appears to be the perfect candidate for the development of large-area graphene based thin films on PET substrate with ultrahigh moisture barrier properties, flexibility and transparency. Seethamraju et al. (2016) synthetized large-area monolayered graphene by chemical vapor deposition, transferred on a polymeric substrate. They reported that reduction of the graphene-embedded polymers was reduced by up to a million-fold, compared to uncoated polymers.

There are many different types of CVD processes: thermal, plasma enhanced (PECVD), cold wall, hot wall, reactive, and many more. The choice of the process depends on the available precursors, the material quality, the thickness, the structure needed and the cost [Ferrari et al. (2014)]. Gas delivery is the main difference in the CVD equipment for the different precursor types. In the case of solid precursors, the solid can be either vaporized and then transported to the deposition chamber, or dissolved using an appropriate solvent, delivered to a vaporizer, and then transported to the deposition chamber. The transport of the precursor can also be aided by a carrier gas [Yan and Xu (2010)]. Depending on the desired deposition temperature, precursor reactivity, or desired growth rate, it may be necessary to introduce an external energy source to aid precursor decomposition [Ferrari et al. (2014)].

One of the most common and inexpensive production methods is PECVD. The creation of plasma of the reacting gaseous precursors allows deposition at lower temperature, compared to thermal CVD. However, since plasma can damage the growing material, is necessary to design the equipment and select process regimes that minimize this damage. The plasma volume reactions are complex because of the large number of different species and possible reaction channels. One important process is the decomposition of the polyatomic carrier gas by electron impact dissociation. The energetic electrons also generate some free radicals and ions that

can decompose the neutral carrier gas and polyatomic radicals by radical–molecule and ion–molecule reactions. The efficiency of the decomposition of the process gas is usually very high. Often, 10 to 100% of the carrier gas fed into the reactor can be decomposed [Tracton (2007)].
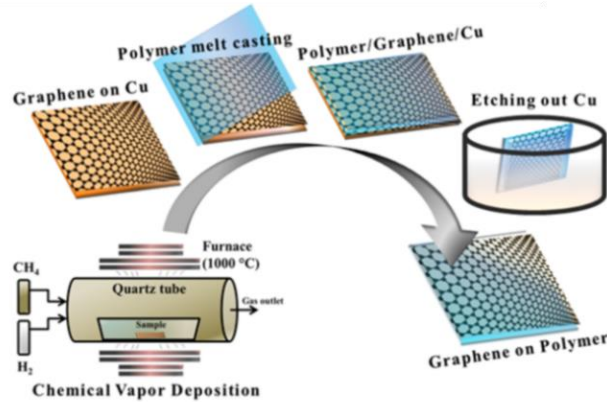
Figure 3.1 Schematic representation of the realization of graphene-embedded polymers by Chemical Vapor Deposition [Seethamraju et al. (2016)].

The formation of the coating takes place on the substrate and on the film surface by absorption of radicals, by chemical bonding to the neighbor atoms on the surface, and by desorption of volatile compounds. The details of the growth process are usually complex, and in many cases not all the reactions are well understood, especially in the case in which more than one chemical compound is involved in the process. The temperature as well as the bombardment of the coating by photons, electrons, and ions can influence the film growth. For technical realization of plasma CVD process, two parts of the deposition system are of great importance, namely, the glow discharge configuration and the gas inlet and distribution system.

The standard equipment for PECVD is a parallel reactor with two electrodes of 10 to 60 cm diameter and a spacing of a few centimeters. The equipment surrounding the reactor depends mainly on the vapor pressure of the precursor. If this is high enough, distillation or sublimation can be simply carried out from a thermostalled reservoir. If the precursor should be heated to reach the required vapor pressure, all tube connections must be heated to avoid condensation. For substances that are difficult to vaporize, the tubes connecting the vaporizer and the reactor should be as short as possible [Tracton (2007)].

PECVD is widely used for the deposition of organic and inorganic thin films on PET substrates with high gas barrier. Wolf et al. (2007) used PECVD to deposit SiN_x thin films in the range of 25-1200 nm on a 100 µm thick PET. At a coating thickness around 25 nm, the water vapor transmission rate was reduced to less than $0.1g/(m^2 day)$. Shirakura et al. (2005) demonstrated that high gas barrier properties against oxygen, carbon dioxide and flavors can be achieved by plasma enhanced CVD of diamond like carbon (DLC) film on PET bottles. Furthermore, the coating exhibited UV barrier, with no impact on the PET bottle recycling. Although DLC-coated PET bottles for hot tea drinks have been sold in the Japanese market, the large-scale PECVD equipment necessary for large-area thin films requires high capital investment, long process time (decreased throughput), and wide space occupation due to pumps and other systems.

3. 2
Wire-Wound Rod Coating

Wire-wound rod coating is a simple technique used to apply liquids to flexible materials in a continuous and control manner. This technique can be used to coat directly onto PET, glass, and other substrates at room temperature and in a scalable way for roll-to-roll production in industry. Rod Coating can be applied in a wide range of fields, such as the manufacture of tapes, labels and flexible packaging, due to the use high precision in the control of the final coating thickness. Wire-wound rods are also called applicator rods, Mayer bars, equalizer bars, coating rods and doctor rods [Tracton (2007)].

The equipment consists in a stainless-steel rod that is wound with a tight spiral of stainless steel wire. A homogeneous solution passes through the groove between the wires, when the rod moves over the substrate. Coating thickness is determined by the cross-sectional area of the grooves between the wire coils of the rod. In figure 3.2 a schematic representation of the rod coating technique is reported.
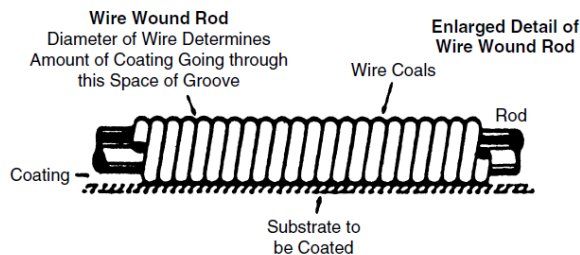
Figure 3.2 Schematic representation of the wire- wound rod coating technique [Tracton et al. (2007)].

Hence, the thickness of the final wet film is directly proportioned to the diameter of the rod's wire. After the passage of the bar over the substrate, the initial shape of the coating is a series of stripes, spaced apart according to the spacing of the groove's wires. Almost immediately, stripes are pulled together by normal surface tension, becoming a uniform wet coating, ready to dry in air or under heat [Wang et al. (2007)]. The thickness of the coating can be influenced from other physical factors,

such as the phenomenon of the shearing action of the liquid. In fact, not all the liquid passes through the groves, but some adheres to the surface of the bar's wire. This phenomenon can influence the thickness of the coating, especially for high viscosity of liquid and when small wires are used. Other factors, such as the speed of the web, web tension, and penetration into the base material influences the thickness.

A lab rod coater is usually equipped with several rods that differ for their wires. To realize a coating, a piece of substrate material is attached to the flat surface of the rod coater, and some coating solution is puddled on the top of the substrate sample. Then, the lab rod that corresponds to the desired thickness is pulled manually or automatically through the liquid. In case of manual rod coater, the quality of the sample can be largely dependent on the skill of the technician. In fact, many factor, such as rod pressure, angle of stoke and speed can cause differences in the thickness and in the appearance of the coating samples [Tracton (2007)].

The main advantage in the use of rod coating is possibility of select the thickness of the coating, choosing the specific bar, without modify the coating solution. Furthermore, rod coating is probably the lowest cost coating technique. However, it is limited to low viscosity coating liquids, that can flow easily between the wire windings, and to flat substrates.

Ferrari et al. (2014) indicated rod coating as one of the most successful deposition techniques for the application of graphene-based coatings on PET substrates. Wang et al. (2007) realized a simple and novel strategy to produce uniform reduced graphene oxide films on a large-scale directly on PET substrates by rod coating. Highly flexible RGO films realized are potentially suitable for various electronic applications, due to their good transparency and low resistance. Su et al. (2014) prepared 30-nm thick RGO coatings onto PET films by rod coating. Moisture barrier of RGO coatings was found to be at least two orders of magnitude better than that provided by Al films of similar thickness.

3. 3
Spray Coating Technologies

Conventional spray coating is widely used for painting in commercial production and is one of the cheapest processes for coating of polymer solutions. It is a high-throughput large-area deposition technique, often used for inline production. This technique ensures ideal coatings on a variety of surfaces with different morphologies, reducing the fluid waste to minimal quantities, and it can access a broad spectrum of fluids with different rheologic behaviors. Hence, deposition by spraying offers the opportunity of tune the system to deposit a wide range of solutions on a wide range of substrates, obtaining the desired product properties [Girotto et al. (2009)]. Spray coating technologies are classified for the quantity of volume deposited and the velocity of the air stream. These parameters influence the deposition efficiency and the quality of the final product. The ability of the operator influences further the quality of the product.

High-volume, low-pressure (HVLP) atomization is a non-conventional spray coating technique that utilizes approximately the same volume of air, compared to conventional spray coating, but a lower pressure to atomize the fluid. This results in a more controlled spray pattern, with the reduction of overspray and "bounce back". Hence, the technique enhances the transfer efficiency of the coating solution, defined as the amount of paint sprayed that goes onto the substrate as compared to the amount lost. High transfer efficiency enhances both productivity and finish quality. In fact, reducing overspray will reduce spray booth maintenance, filter replacement, waste disposal and material costs. HLVP presents a transfer efficiency from 65% to 85%, compared to conventional spray with an efficiency from 30% to 40%.

In general, HVLP can be used with most low-to-medium solids materials including two-component paints, urethanes, acrylics, epoxies, enamels, lacquers, stains, and primers. Some HVLP application equipment can atomize higher viscosity materials and/or higher fluid flow rates. HVLP spray equipment consists of a high-volume air source, a material supply system and a HVLP spray gun, as reported in figure 3.3. Different types of air source and material supply systems are available for HVLP spray, providing a wide range of delivery volumes and pressures [Tracton (2007)].

In literature, spray coating technology is widely used to improve gas barrier properties of PET. Layek et al. (2014) developed a very simple and inexpensive method for the preparation of super hydrogen barrier PET film, spraying a layer structured graphene oxide(GO)/polyvinyl alcohol (PVA) coating on a PET surface.
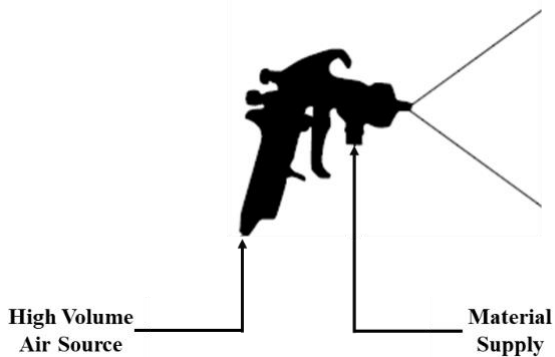
Figure 3.3 Schematic representation of the High Volume Low Pressure Spray Coating.

The gas barrier properties of the GO/PVA coated PET sample increased dramatically compared to uncoated samples and they increased with the increase of the amount of coating solution. Kim et al. (2016) fabricated, by spray coating, a high-performance oxygen gas barrier coating on PET, alternately stacking negatively charged graphene oxide and positively charged amino-ethyl-functionalized GO (AEGO). One layer of GO/AEGO/GO stacked film coated on a PET substrate showed an oxygen permeability of 0.01 cc/m^2 day atm, which is 10^3 times lower than that of pure PET.

CHAPTER

4

Development of the water vapor barrier coating matrix

In this chapter, the development of the water vapor barrier coating is illustrated. The polymer (HAVOH) used as starting point for the design of the coating is first presented (§4.1). Because of similarities between HAVOH and PVA, possible crosslinking agents for HAVOH are selected in PVA crosslinking literature (§4.2). Then, tests are performed to establish the successful crosslinking reactions on HAVOH for the selected crosslinkers (§4.3 ████████████████████████████████ ████████████████████████████████ ████████████████████████████████ ████████████████████████████████ *The industrial feasibility of the developed coating is confirmed performing three simple lab-scale (§4.7). Finally, future developments to complete the design of the coating are hypothesized (§4.8).*

HAVOH as starting point for the design of the barrier coating matrix

The first step of the moisture barrier coating design is the choice of a polymer that should be modified to achieve the high moisture barrier effect. The polymer to use as starting point should show several properties needed for packaging, such as high transparency, stability in water solution and ease of coating on PET surfaces. One of the polymeric material that meets these requirements is High Amorphous Vinyl Alcohol (HAVOH).
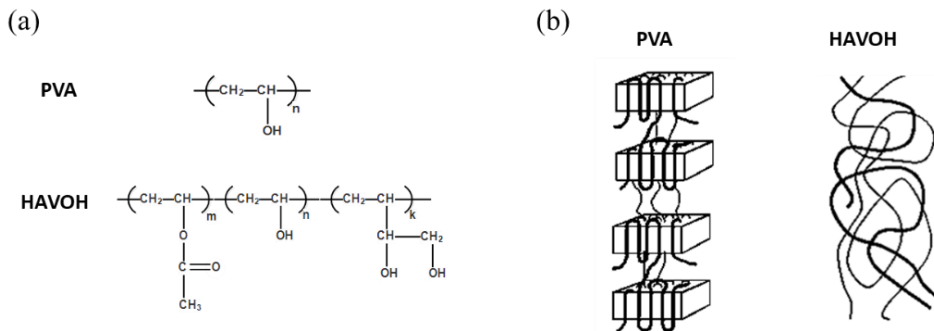
Figure 4.1 (a) Chemical formula of PVA and HAVOH; (b) schematic representation of semi crystalline structure of PVA and amorphous structure of HAVOH.

HAVOH is a novel biodegradable polymer based on modified PVA, patented by Nippon-Goshei (Japan) and commercialized with trade name of Nichigo G-Polymer. Compared to PVA, the chemical formula of HAVOH, reported in figure 4.1(a), shows the presence of ester groups that inhibit the formation of crystalline regions. The low crystallinity and the high hydrogen bonding strength give to HAVOH several advantages, including low melting points, high stretching characteristics and high gas barrier performance, as well as low foaming, aqueous solution stability and emulsification performance [Donato et al. (2016)]. In table 4.1, an overview of HAVOH properties, compared to PVA and EVOH, is reported.

HAVOH starts to be used in literature, due to its high gas barrier properties and ease of processing. Donato et al. (2016) realized HAVOH-silica bio-nanocomposites using ionic liquids as additives. Simple sol-gel approach used for the realization of these hybrid structures allowed a significant decrease of water vapor permeability and an increase of storage and tensile modulus.

Table 4.1 Main properties of HAVOH compared to PVA (fully and partially saponified) and EVOH [source Nippon-Goshei].

Properties	PVA (partially saponified)	PVA (fully saponified)	EVOH	HAVOH
Extrudability	✔		✔	✔
Excellent stretchability	✔			✔
High gas barrier		✔	✔	✔
Low foaming		✔		✔
Emulsifiability	✔			✔
Water solution stability	✔			✔
Biodegradability	✔	✔		✔

Yan et al. (2015) used HAVOH as one of the compounds of their multilayer structure to apply on PET for the improvement of oxygen barrier properties. They showed that 40 layers of HAVOH/zyrconium oxynitrate hydrate /reduced graphene oxide ultrathin films deposited on PET lead to a decrease of one order of magnitude of oxygen permeability with respect to the pristine PET substrate.

The limit of the use of HAVOH in packaging is its high solubility in water. This makes difficult to apply HAVOH in cases in which water is involved. For this reason, is necessary to achieve the insolubility in water by chemical crosslinking of HAVOH. The chemical crosslinking decreases the quantity of -OH groups on

polymer chain, responsible of the interaction with water. The approach of removing -OH groups to increase the insolubility of a polymer is widely used in literature, especially to increase the insolubility of PVA. Hence, a strategy to find possible crosslinking agents for HAVOH should be the investigation of crosslinking agents and methods used in literature for PVA.

4. 2

PVA crosslinking methods

Poly vinyl alcohol (PVA or PVOH) is a water soluble synthetic polymer, produced from the hydrolysis of polyvinyl acetate (PVAc). By controlling hydrolysis step, different grades (as degree of hydrolysis [DH]) of PVA polymer can be prepared and finally affect the behavior of polymer material, solubility, crystallinity, and chemical properties [Kumar and Han (2017)]. Nowadays, researchers have given more and more attention to its utilization in several applications, especially in medical, pharmaceutic and packaging field.

PVA has unique properties, such as thermal resistance, resistance to chemicals, film and coating forming ability, transparency and good mechanical properties. Furthermore, it is nontoxic, biodegradable and biocompatible. However, other properties, such as excellent hydrophilicity and high degree of swelling, limit the use of PVA in applications in which water is involved. To increase the fields in which PVA can be applied, plenty works has been done and a lot of solutions have been proposed. These solutions include freezing, heat treatment, irradiation, and chemical crosslinking [Bolto et al. (2009)].

Freezing of PVA membranes can induce the formation of crystalline regions in their morphology. The induced crystalline regions can physically crosslink PVA, as demonstrated by the reduction of swelling degree with increase of crystallinity [Ofsted and Poser (1989)]. Increase of crystallinity of PVA can be achieved further by a heat treatment. Xianda et al. (1987) demonstrated that PVA treated at temperatures up to 160°C shown a decrement of hygroscopicity and water vapor permeability. The decrease of swelling in water can be achieved by the ionizing radiation of PVA films. The swelling ratio (swollen mass/dry mass) of the samples in water was lowered from 5.7 to 2.6 by the irradiation treatment [Katz and Wydeven (1981)].

Among solutions discussed, chemical crosslinking has been proved an effective way to improve the specific properties of PVA, reducing the solubility in water and the degree of swelling. A wide range of chemical compounds can crosslink PVA, forming hydrogen or covalent bonding with -OH groups of the polymer chain, reducing their affinity with water. In the case of covalent bonding formation, PVA can be chemically crosslinked by acetalization with formaldehyde and

glutaraldehyde or by esterification with L-maleic acid, citric acid and fumaric acid [Gao et al. (2016)]. PVA chemical crosslinker can be classified in four main categories: metal ions, poly carboxylic acids, aldehydes, and blend polymers.

Metal ions often behave as crosslinking centers between polymers when the polymer possesses the ability to form metal–polymer complexes. Random crosslinking across polymer chains entraps water in growing three-dimensional networks, which can convert the system into a dense and uniform structure with few defects. Lee et al. (2014) realized a PVA/ZrO$_2$-based composite coating, using a water solution of PVA and Zirconium Oxynitrate Hydrate to apply on stainless steel to improve the corrosion protection. Yan et al. (2015) hypnotized that zirconium-based compounds are valuable crosslinking agents because of their strong ionizable nature in a water solution and intrinsic capability to promote intermolecular interactions via hydrogen and covalent bonds.

Poly carboxylic acids are widely used in literature to crosslink PVA. Gao et al. (2016) investigated the effect of the crosslinking by L-maleic acid on the hygroscopic performance of PVA films. They analyzed the effect of the concentration of L-maleic acid and of the thermal treatment on the swelling, demonstrating that the high crosslinking degree, due to the esterification of PVA, can decrease membrane swelling. Stone et al. (2013) prepared PVA/Alginate nanofiber hydrogels by in situ crosslinking using citric acid followed by curing at 140°C for 2 h and conditioning at room temperature. As prepared crosslinked nanofibers showed enhanced thermal stability and insolubility (remained intact) in water for two days. Furthermore, no significant change in the mechanical performances of the crosslinked PVA/Alginate was observed after repetitive water immersion and drying cycles. Birck et al. (2014) studied the effect of the citric acid concentration and crosslinking thermal treatment on antimicrobial properties of PVA, considering citric acid as a low cost, non-toxic crosslinker ideal for the food packaging application.

Aldehydes, such as Formaldehyde [Chen et al. (1973)], bond easily to PVA, but exhibit some toxicity and high cost, which limits their further application. Conversely, bi-functional aldehydes, especially Glutaraldehyde, are the preferred crosslinking agents, due to their low cost, commercial availability, good reactivity and very low toxicity. Marin and Rojas (2015) evaluated the effect of PVA-Glutaraldehyde ratio, pH and crosslinking reaction time on the physicochemical and water sorption properties of the resulting crosslinked PVA film. The chemical reaction between PVA and Glutaraldehyde modified the original polymer chain by reducing wettability, water sorption and solubility, due to the formation of several

acetal bonds. The crosslinking reaction caused also the reduction of hydroxyl network and crosslinked films resulted more amorphous.

PVA can be blended with other polymers, such as poly (acrylic acid) PAA, and crosslink forming covalent bonds. Lim et al. (2016) prepared five crosslinked PVA/ PAA blends to enhance oxygen barrier and water resistance of PVA. With increasing of PAA content, the crosslinking density was significantly increased, resulting in changes in the chemical structure, morphology and crystallinity of the films. The oxygen transmission rate of pure PVA decreased from 5.91 to 1.59 $g/(m^2 \text{ day})$ with increasing PAA ratio. Moreover, the water resistance increased remarkably, with no impact on the good optical transparency of PVA.

4. 3
Crosslinking agent selection for HAVOH

██
██████████

██
██
██
██
██████████████████████████████

4.3.1 FTIR Analysis

██
██
██
██
████████████████████

██
██
██
██
██
██
██
██

██
██
██
██
██

██
██
██
██
██████████████████████████

4.3.2 UV-Vis Analysis

███
██████████████████████████████████

4.3.3 Hot Water Tests

██
██
██
██
██
██
██
██
███

44

4. 4

███

██
██
██
███

4.4.1 Swelling Tests

██,
██
██
██
██
██
██
███████████████████████████████████

██

██
██
█████████████████████████

██

██
██
██
██████████████████████████

██
██

██
██
██
██
██
██
███████████████████████████████

4.4.2 FTIR Analysis

██
██
██
██
███
██
██

4.4.3 UV-Vis Analysis

4.4.4 WVTR tests

███
██
███████████████████████

██
██
██

███
██
██
██
██
██

███
███
████████████████████
    ██
███
██

███
            ████████████████████

    ██
███
███

    ██

4. 5

██

███
███
███
███
███████████████████

4.5.1 Swelling Tests

███
███
██

██
██████████████████

4.5.2 FTIR Analysis

███
███
███
███
███████████████████████████

███
███
███
███
███
███
███
███
████████████████████████████████████

██
██
██
██
██
██
██
██
██
██
██
██
██

██
█████████████████████████████

4.5.3 UV-Vis Analysis

4.5.4 WVTR tests

███████████████████████████████████████

███

██

██

███

███

███

███

██

████████████████████████████████████

██

█████████████████████████████████████

4. 6

Considerations on HAVOH-based coating developed

4.7
From Lab-Scale to Industrial Process

██
███
███
███
███
███████████████████████████

4.7.1 Coating configuration

███
██████████████████████████████████████
███
███
███
██████████████████████████████████████

███
███

███
███

██
██

4.7.2 Linkage between coated PET bottles

██
██
██████████████████████████

██
██

4.7.3 Recyclability of the developed coating

Among rigid plastics, PET usually represents one of the most frequent type of

4. 8
Future Developments

CHAPTER

5

Evaluation of 2D-additives

In this chapter, the selection of possible 2D-additives for developed moisture barrier coating is performed, considering graphene-based additives. First, the influence of impermeable sheets on gas transport in polymers is theoretically explained (§5.1). Then, results obtained loading developed coating solution with graphene (§5.2), graphene oxide (§5.3), and reduced graphene oxide (§5.4) are presented. Lastly, consideration and future developments on the use of additives in the developed coating are illustrated (§5.5).

The importance of
graphene-based additives

Developed moisture barrier coating exhibits high water vapor barrier effect with a coating thickness of 35 µm on PET. Probably, this coating thickness is too high to be obtained during a fast-industrial process. In fact, to achieve a 35µm-thick coating, probably more successive layers of the developed solution should be applied one the PET bottles, delaying their production. To decrease the thickness of the coating preserving the water vapor barrier effect, is potentially possible to disperse impermeable additives in the coating matrix, such as graphene-based additives. The role of the graphene-based additives is to increase the tortuosity of the diffusion path of gas molecules across the coating matrix, as illustrated in figure 5.1.

Graphene-based additives, such as graphene, graphene oxide and reduced graphene oxide, compared to impermeable inorganic additives, present higher aspect ratio (α) that increase further the gas molecules path [Yoo et al. (2014)].
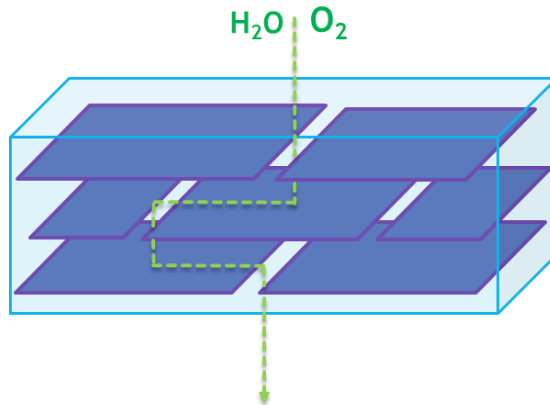
Figure 5.1 Barrier to permeation imposed by nanoparticles imbedded in a polymeric matrix.

Nielsen (1967) proposed a simple model that includes impermeable inorganic platelets in a permeable matrix. According to the solution–diffusion model, the gas

permeability in polymer membranes can be expressed as a product of the diffusivity and solubility as follows:

$$P = DS \tag{5.1}$$

where P is the gas permeability of the polymeric coating, D is the diffusivity of the gas molecules through the coating, and S is the solubility of the gas molecules in the coating. The solubility of nanocomposites can be expressed as a function of the volume fraction of the filler as follow:

$$S = S_0(1 - \varphi) \tag{5.2}$$

where S_0 is the solubility of the pure polymer matrix and φ is the volume fraction of the impermeable fillers. The diffusivity of nanocomposites can be expressed with tortuosity as follows:

$$D = D_0/\tau \tag{5.3}$$

where D_0 is the diffusivity of the pure polymer matrix. Tortuosity (τ) is defined as:

$$\tau = l/l' \tag{5.4}$$

where l' is the distance between tortuous pathways through the membrane and l' is the membrane thickness, that is, the shortest pathways for gas molecules [Choudalakis and Gotsis (2009)]. From equations (5.1), (5.2), and (5.3):

$$P/P_0 = (1 - \varphi)/\tau \tag{5.5}$$

where P_0 is the gas permeability of pure polymer matrix. If N is defined as the average number of inorganic platelets,

$$l' = l + N \cdot L/2 \tag{5.6}$$

Because of $N = l(\varphi/W)$, τ can be rewritten as follow:

$$\tau = 1 + \frac{L}{2W} \cdot \varphi \tag{5.7}$$

From equations (5.5) and (5.7),

$$P/P_0 = (1 - \varphi)/(1 + \frac{\alpha}{2}\varphi) \tag{5.8}$$

where $\alpha = L/W$ is the aspect ratio of the impermeable sheets . This equation can be used only when $\varphi \leq 0.1$ because the impermeable inorganic fillers tend to aggregate with increasing φ [Choudalakis and Gotsis (2009)]. The predicted gas permeation models for different α are presented in figure 5.2(a):
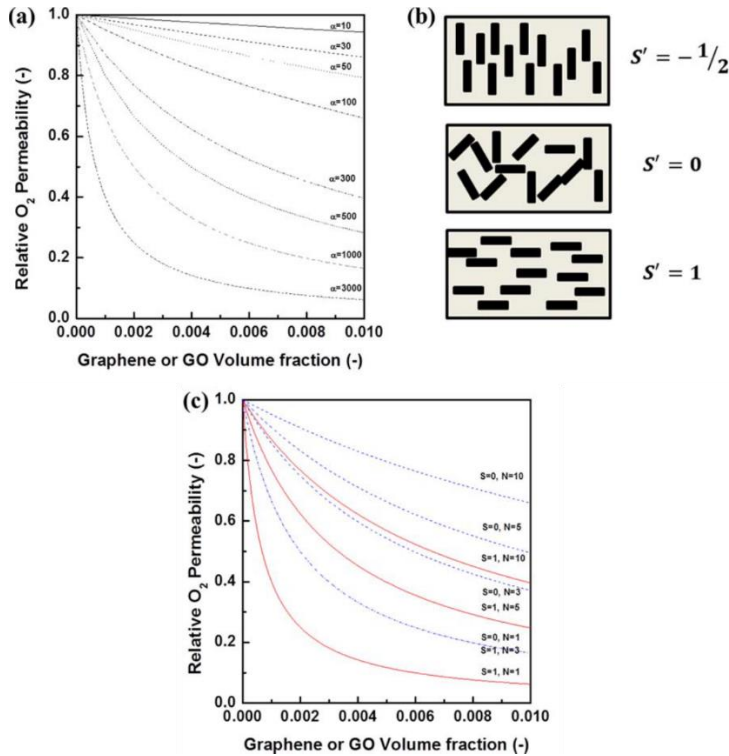
Figure 5.2 Gas transport in graphene/polymer nanocomposites: (a) effect of the graphene nanoplatelet size, (b) S' for the orientations of graphene nanoplatelets in the polymer matrix, and (c) effect of the orientation and the number of graphene nanoplatelet layers (α=3000) [Yoo et al. (2014)].

The stacking orientation of graphene layers in a polymer matrix and self-aggregation of graphene nanoplatelets are important factors influencing the gas permeability of nanocomposites [Choudalakis and Gotsis (2009)]. Nielsen's equation [Nielsen (1967)] is expressed as follows:

74

$$\frac{P}{P_0} = \frac{(1-\varphi)}{1+\frac{\alpha}{2}\frac{2}{3}(S'+\frac{1}{2})\varphi} \tag{5.9}$$

where S' is the order parameter representing orientations of inorganic platelets, as presented in figure 5.2(b). In the case of a high filler loading, equation (5.8) can be rewritten with consideration of the degree of stacking with the parameter N [Kim and Macosko (2009)]. Therefore, the equation can be expressed as follows:

$$\frac{P}{P_0} = \frac{(1-\varphi)}{1+\frac{\alpha}{2N}\varphi} \tag{5.10}$$

From equations (5.8) and (5.9),

$$\frac{P}{P_0} = \frac{(1-\varphi)}{1+\frac{\alpha}{3N}(S'+\frac{1}{2})\varphi} \tag{5.11}$$

As shown in figure 5.2(b), polymer/inorganic nanocomposites are supposed to have three types of orientations corresponding to three S'. With the supposition that gas transport occurs between graphene nanoplatelets and the polymer, a main factor in improving the gas-barrier properties in polymer nanocomposites will be the tortuosity. For S'=1, that is in the case of a horizontally stacked structure, graphene nanoplatelets can maximize the tortuosity, decreasing significantly the gas permeation rate through the resulting nanocomposites [Choudalakis and Gotsis (2009)]. However, when the degree of nanoplatelet stacking (N) is increased, the overall tortuosity of the polymer matrix will much lower; therefore, the barrier properties of the polymer nanocomposite will be relatively low. The predicted gas permeance results for different N and S' values when α=3000 are shown in figure 5.2(c).

As graphene nanoplatelets tend to aggregate, that is as the value of N is increased, the gas-barrier properties significantly decline. This is because the aggregated graphene or GO nanoplatelets increase the probability that gas molecules flow through the relatively highly permeable polymer matrix rather than graphene or GO as compared with a well-dispersed and exfoliated graphene/polymer nanocomposite with same volume fraction of graphene or GO. These phenomena are related to the compatibility in the interfaces between the polymer and GO. The polar groups of GO basically provide compatibility with the polymer. Well-dispersed GO shows high compatibility because of biplanar polar groups; therefore, this also indicates an improved gas-barrier performance with long diffusional pathways.

Aggregated GO platelets, however, show reduced compatibility with the polymer matrix, and thus, the polymer exhibits a low gas-barrier performance with decreased diffusional pathways. In the case of a fully exfoliated (N=1) and horizontally stacked (S'=1) graphene in a polymer matrix, an only 1 vol% addition of graphene nanoplatelets can reduce the gas permeability by a factor of 10 relative to that of the pure polymer matrix. However, in the case of 10-layer-stacked (N=10) and randomly oriented (S'=0) graphene in a polymer matrix, 1 vol% graphene nanoplatelets show only a 30% reduction in the original gas permeability. Accordingly, the orientation and the degree of exfoliation are very important for achieving improved gas-barrier properties in graphene/polymer nanocomposites [Yoo et al. (2014)].

On the basis of these considerations, the use of graphene-based additives well dispersed in the developed coating matrix can increase further its water vapor barrier effect.

5. 2

Graphene Additives

Graphene is the name given to a flat monolayer of carbon atoms tightly packed into a two-dimensional (2D) honeycomb lattice, and is a basic building block for graphitic materials of all other dimensionalities. It is a 2D allotrope of sp^2 carbon in the form of a planar monolayer. Compared with other nanomaterials, graphene is structurally unique, whereas the lateral dimensions of graphene are up to 10s of micrometers or larger, and the thickness is at the atomic scale.

Since Geim and Novoselov (2007) reported monolayer graphene mechanically exfoliated from graphite, graphene has gained interest because of its many unique properties. In fact, graphene is known as the strongest material ever measured, with a Young's modulus of 1 TPa [Jiang et al. (2009)]. It exhibits a high thermal conductivity of 5300 W m^{-1} K^{-1} [Balandin et al. (2009)], and an extremely high surface area of 2630 m^2/g [McAllister et al. (2007)]. Furthermore, graphene has a high electron mobility of 200,000 cm^2 V^{-1} s^{-1} [Bolotin et al. (2008)], and an electrical conductivity of up to 1000 S/cm [Wu et al. (2008)].

Gas barrier properties of graphene are interesting likewise. In fact, it is known as a soft, 2D crystal material that is impermeable to any gas molecules. The electron density of aromatic rings in graphene is high enough to repel the penetration of atoms or molecules. Leenaerts et al. (2008) demonstrated that a monoatomic molecule of helium (He) can be reflected by a non-defective graphene monolayer. In fact, they calculated that the kinetic energy of the He atom (18.6 eV) is smaller than the energy barrier penetration (18.8 eV). However, is not easy to synthetize large-area, defect-free graphene sheets because there are some defects due to the graphene boundaries, point defects and carbon rings with more or less than six carbon atoms. These defects decrease the energy barrier of graphene sheets [Leenaerts et al. (2008)].

Hence, the big challenge is to develop new effective and scalable approach to produce non-defective graphene layers. Currently, there are six main techniques to prepare graphene: chemical vapor deposition [Eizenberg and Blakely (1979)], epitaxial growth [Berger et al. (2006)], cutting nanotubes [Jiao et al. (2009)], liquid phase exfoliation [Ferrari et al. (2014)] and reduction of graphene oxide [Gao et al. (2010)]. Each of these techniques differs for the quality of graphene produced and for level of feasibility in a large-scale production.
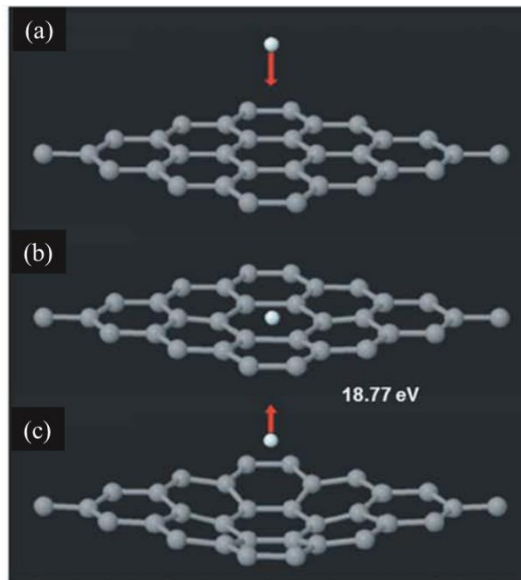
Figure 5.3 Reflection of an He atom with a kinetic energy of 18.6 eV from a graphene surface: (a) The He atom approaches the perfect graphene layer. (b) The He atom comes to rest before penetrating the graphene layer; the relaxation of the graphene layer is very small at this moment. (c) The He atom is reflected back, and the surface starts to relax [Yoo et al. (2014)].

In this context, liquid phase exfoliation of graphene is recently attracting huge scientific and industrial attention because it is a low-cost and scalable process exhibiting high-throughput potential, as well as the possibility of integration with other processes [Paton et al. (2014)]. Furthermore, it is the ideal technique for coating solutions based on graphene [Ferrari et al. (2014)]. In these solution-based techniques, graphene powder is dispersed in organic solvents or aqueous surfactant solutions. Shock waves and cavitation generated by sonication and shear produced by a rotor break apart the graphite flakes into small particles as single layer graphene and few layers of graphene [Nicolosi et al. (2013)]. After removing the larger particles by centrifugation, a homogeneous liquid dispersion of few layers graphene and monolayers of graphene is obtained.

The surfactant chosen for the exfoliated graphene solution should not affect graphene properties. It has been stated that in order to increase yield, surface energy (δS) of exfoliating solutions should be similar to that of graphene at 46.7mN/m [Pu et al. (2012)].

5.2.1 ███
███████████████

██
██
██
██
██
██
██
█████████████████████

██
██
██
██
██
███

5.2.2 WVTR and OTR tests

██
██
██
██
██
██
██
████████████████████████████████████

██
██
██████████████████████████████████████

Graphene Oxide Additives

Graphite oxide is the product of the oxidation of graphite, and exhibits plane of carbons decorated by oxygen-containing groups. These groups expand the interlayer distance and make the atomic-thick layers hydrophilic. As a result, these oxidized layers can be exfoliated in water under moderate ultrasonication. If the exfoliated sheets contain only one or few layers of carbon atoms like graphene, these sheets are named graphene oxide (GO) [Novoselov et al. (2004)].

Although the precise chemical structure of GO is still not quite clear, the widely accepted GO model was proposed by Lerf and Klinowski, that hypothesized a nonstoichiometric model, illustrated in figure 5.5, where the carbon plane is decorated with hydroxyl and epoxy (1,2-ether) functional groups. Carbonyl groups are also present, most likely as carboxylic acids along the sheet edge but also as organic carbonyl defects within the sheet [Lerf et al. (1998)] [He et al. (1998)].

Carboxylic acid groups at the edges of the GO planes help to stabilize the colloidal state of a GO suspension in some polar solvent without any surfactant. For example, is possible to achieve fully exfoliated GO suspension in water, by ultrasonication [Demazeau (1998)].
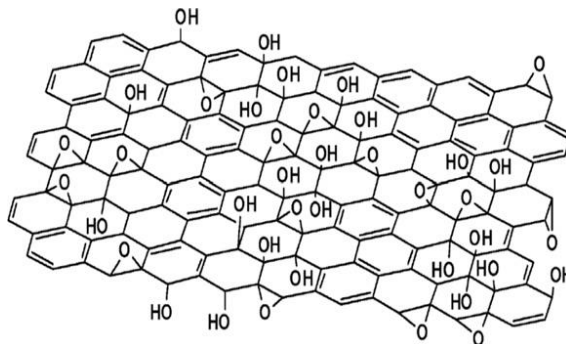
Figure 5.5 Lerf–Klinowski model of GO with the omission of minor groups (carboxyl, carbonyl, ester, etc.) on the periphery of the carbon plane of the graphitic platelets of GO [Lerf et al. (1998)] [He et al. (1998)].

Hummers and Offeman (1958) proposed a new synthesis method for the oxidation of graphite with potassium permanganate (KMnO4) and concentrated sulfuric acid as oxidizing agents. After these studies, the Hummers method and its modified methods have been widely adapted for synthesizing GO.

The main advantage of the use of graphene oxide as additive in coatings is that it can be produced using inexpensive graphite as raw material by cost-effective chemical methods with a high yield. Furthermore, it is highly hydrophilic and can form stable aqueous colloids to facilitate the assembly of macroscopic structures by simple and cheap solution processes.

Graphene oxide is widely used in literature as additive to improve mechanical and barrier properties of polymers. Loryuenyong et al. (2015) prepared PVA-graphene oxide and PVA-graphite oxide composites that improved both mechanical properties, with an increase of the elastic modulus of 144%, and oxygen barrier properties, with an oxygen transmission decrease of 76%. Lai et al. (2015) performed a bio-inspired method to realize composite films based on PVA crosslinked by borate ions and graphene oxide. PVA/GO films with only 0.1%wt GO and 1%wt of crosslinker exhibited an oxygen transmission rate lower than 0.005 g m^{-2} day $^{-1}$.

5.3.1 ███

███████████████████████████████████

██
███
███
███
███
███
██
███
██
██████████████████████████████████.

5.3.2 WVTR and OTR tests

<div align="right">

5.4

</div>

Reduced Graphene Oxide Additives

Graphene oxide, due to its hydroxylic behavior, is not appropriate as additive to prevent water vapor transmission. To change the behavior of GO from hydroxylic to hydrophobic, is necessary to reduce all oxygen functionalities present on basal planes, responsible of the GO sensitivity to moisture. Reduced graphene oxide (RGO) composites are able to decrease both oxygen and water vapor transmission rate. Yan et al. (2014) realized natural rubber-RGO composites via latex mixing and co-coagulation approach followed by static hot-press and twin roll mixing process. Composites with RGO segregated network exhibited both barrier to oxygen and water vapor permeation and mechanical properties improved with respect to pristine rubber and composites with the homogeneous dispersion of single RGO platelets. Kim et al. (2011) realized PVA-RGO composites, synthesized by solution mixing method and performing chemical reduction using hydrazine monohydrate. The oxygen permeability of the PVA/RGO (0.3 wt.%) composite coated film was 86 times lower than that of the pure PET film, with 73% light transmittance at 550 nm.

In literature, several methods for the reduction of the graphene oxide are illustrated. None of reduction methods reported allows the complete removal of oxygen functionalities from the basal plane of graphene oxide. In fact, the reduction allows to a partial restoring of sp^2-conjugated graphene network. These methods can be classified in three main categories [Yoo et al. (2014)]: thermal reduction, irradiation-assisted reduction, and chemical reduction.

Thermal reduction is usually performed above 200°C in vacuo [Becerril et al. (2008)] and in an inert atmosphere [Wang et al. (2008)]. Typically, a more efficient reduction can be achieved at high temperatures because some oxygen functional groups can gradually decompose at temperatures above 200°C [Stankovich et al. (2007)]. Thermal reduction allows to an RGO full of structural defects, which results in notable water permeation. In fact, the reduction by thermic treatment causes vacancies in the basal plane because of the evolution of carbon in the form of CO or CO_2 [Schniepp et al. (2006)].

UV-assisted photocatalytic reduction and microwave-assisted reduction are also used for GO reduction. Wu et al. (2011) verified that a stable water dispersion of RGO is produced by UV irradiation of a GO solution in presence of n,n-

dimethylformamide(DMF). Rapid and reduction of graphene oxide (GO) to graphene can be achieved with the assistance of microwaves in a mixed solution of n,n-dimethylacetamide (DMAc) and water. The reduction time is found to be in the scale of minutes. The as-prepared graphene can be well dispersed in DMAc/water solution to form an organic suspension, and the suspension is stable for months at room temperature [Chen et al. (2010)].

Chemical reduction is the most used reduction method in literature because is possible to produce RGO with low number of defects. Furthermore, chemical reduction can be achieved in both the liquid and the gases [Yoo et al. (2014)]. Chemical reduction agents include hydrazine [Gomez-Navarro et al. (2007)], metal hybrids [Mohanty et al. (2010)], ascorbic acid [Fernández-Merino et al. (2010)], and Hydrogen Iodide gas [Moon et al. (2010)]. A schematic representation of the chemical reduction of GO is illustrated in figure 5.7.
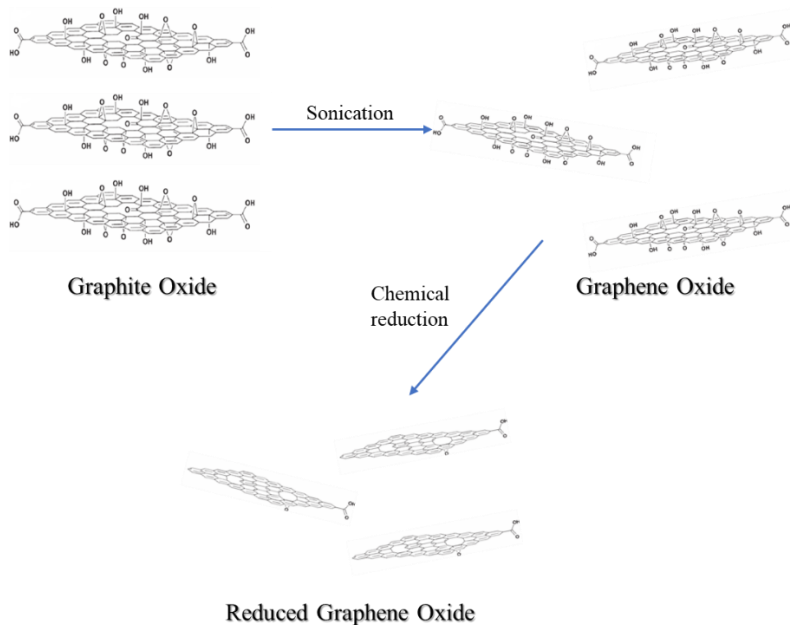
Figure 5.7 Schematic representation of the chemical reduction by graphene oxide to reduced graphene oxide.

Hydrazine is one of the most efficient chemical reducing agents for graphene oxide, but the use of such reagent in the large-scale implementation is not desirable due to its high toxicity. Moreover, it is potentially explosive. In the search for

alternatives to hydrazine, two relevant factors should be considered, in addition to environmental and safety issues. First, the process should be at least as effective as hydrazine in the deoxygenation of graphene oxide. Second, the reduced material should remain dispersed as single-layer sheets in aqueous and organic media; that is, it should not precipitate after reduction.

Fernández-Merino et al. (2010) found that the efficiency of hydrazine in the reduction of graphene oxide is matched by ascorbic acid (Vitamin C), a nontoxic and natural antioxidant essential for many metabolic function in living organism. Zhang et al. (2010) demonstrated the successful reduction of graphene oxide by ascorbic acid, considering color shift of GO solution. In fact, when reduction occurs, the color of solution changes from yellow/brown, that is the typical color of graphene oxide, to black, that is the typical color of reduced graphene oxide.

5.4.1 Ascorbic acid as reducing agent for graphene oxide

The agent chosen for the reduction of graphene oxide is ascorbic acid. great advantage in the use of this chemical agent is its non-toxicity in contrast to hydrazine. The mechanism for the chemical reduction is still an open question, but it can be speculated as two-step S_N2 nucleophilic reactions, followed by one step of thermal elimination.

This hypothesized mechanism is reported in figure 5.8. The electron withdrawing five-membered ring of L-ascorbic acid makes hydroxyls more acidic, so L-ascorbic acid is ready to dissociate two protons, functioning as a nucleophile. Graphite oxide contains mainly two types of reactive species on its basal plane, including epoxide and hydroxyl. In the case of epoxide, it could be opened by the oxygen anion of L-ascorbic acid (HOAO$^-$) with a S_N2 nucleophilic attack. The reduction may be followed by a back-side S_N2 nucleophilic attack with release of H_2O, resulting in the formation of an intermediate. Finally, the intermediate may undergo a thermal elimination, leading to formation of reduced graphene. The ascorbic acid is oxidized into dehydroascorbic acid. The reduction of hydroxyls is similar to the case of epoxide. The hydroxyls could be displaced by the oxygen anions of L-ascorbic acid ($^-$OAO$^-$) with a back-side S_N2 nucleophilic attack twice, which are subsequently reduced further by thermal elimination [Gao et al. (2010)].
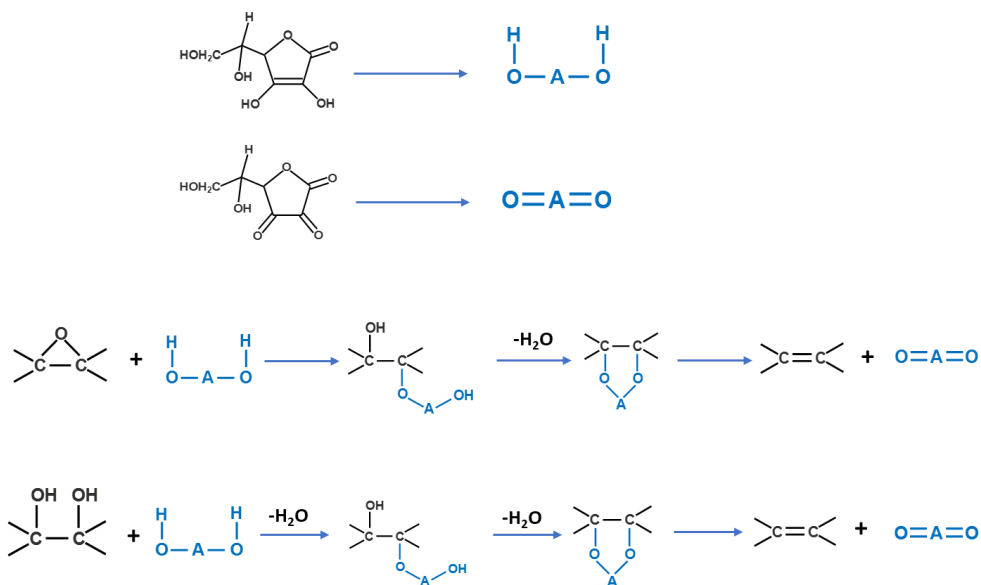
Figure 5.8 Proposed mechanism of reaction for the reduction of graphene oxide by L-ascorbic acid.

Optical observation is a direct way to see the changes in GO, before and after the reduction by ascorbic acid. In fact, in the case of reduction of GO films, since the reduction process can drastically improve the electrical conductivity of GO, the increased charge carrier concentration and the mobility will improve the reflection to incident light, which makes RGO films have a metallic luster compared to its GO film precursor, with a brown color and semi-transparency. Instead, in the case of reduction in colloidal state, chemical reduction usually results in a black precipitation from the original yellow-brown suspension, probably attributable to the increase in the hydrophobicity of the material caused by a decrease in the polar functionality on the surface of the sheets [Pei and Cheng (2011)].

To evaluate the minimum quantity of ascorbic acid for the reduction of GO, reduction was realized, with the following method, and color shift and precipitation of RGO were evaluated, as confirm of the successful reduction.

A water suspension of GO (0.1mg/ml) was prepared dispersing GO powder in distilled water by sonication for 2h. The solution was divided in four equal part and ascorbic acid powder, at four different ratio L-AA/GO g/g (10:1, 20:1, 30:1, 40:1). Solution were stirred at 90°C for 1h, and the shift color from brow to black was observe in all solutions.
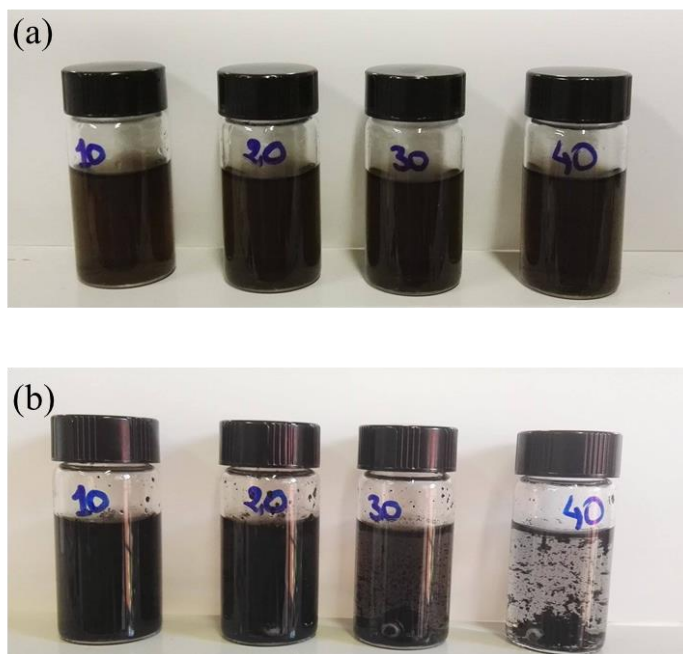
Figure 5.9 GO water dispersion (0.1mg/ml) before (a) and after (b) reduction by four different quantities of L-ascorbic acid.

As is possible to observe in figure 5.9, the quantity of RGO precipitated in water increase with the L-AA/GO ratio. This is attributable to an increase of the quantity of GO reduced in solution. In fact, observing solution with L-AA/GO ratio 10:1, 20:1, 30:1, unreduced GO is still dispersed in solution, while reduced GO precipitates. Instead, in the case of 40:1 L-AA/GO ratio, all graphene oxide seems to be precipitated, due to the effect of reduction.
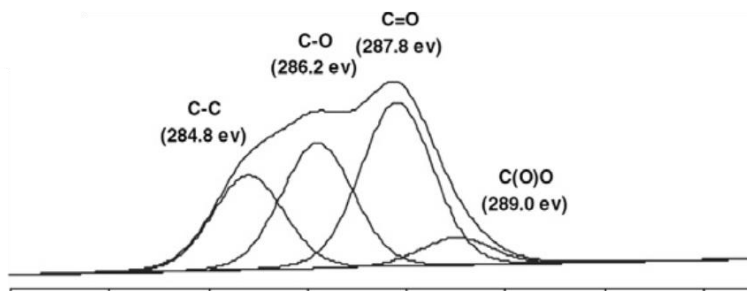
Figure 5.10 The C1s spectrum of GO [Pei and Cheng (2011)].

In figure 5.10, the C1s XPS spectrum of GO is reported, indicating a considerable degree of oxidation with four components that correspond to carbon atoms in different functional groups: the non-oxygenated ring C (284.6 eV), the C in C–O bonds (286.0 eV), the carbonyl C (287.8 eV), and the carboxylate carbon (O–C = O, 289.0 eV) [Pei and Cheng (2011)].
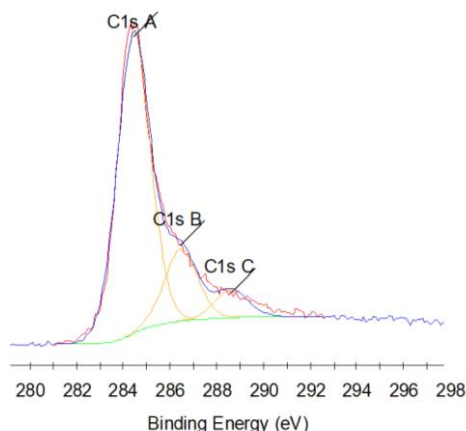
Figure 5.11 The C1s spectrum of RGO (L-AA/GO ratio 40:1).

To evaluate the reduction of GO using 40:1 L-AA/GO, XPS analysis were performed. As demonstrated in the C1s XPS spectrum reported in figure 5.11, RGO exhibits these oxygen functionalities, reported as C1s B, corresponding to the C in C–O bonds, and as C2s C, corresponding to carboxyl groups. These peaks result much weaker, that in GO spectrum.

5.4.2 In-situ reduction procedure

For the preparation of coating based on HAVOH and RGO, two procedures were performed. These two procedures differ in terms of reduction of GO, that can occur in the coating solution (in-situ) or outside the coating solution (ex-situ).

In-situ reduction procedure scheme is reported in figure 5.12. First, a stable dispersion of GO is prepared sonicating GO powder in water until all the powder is dispersed (step 1). Then, HAVOH powder is dissolved in GO solution at 90 °C for 2h (step 2). Adding L-ascorbic acid solution (L-AA/GO ratio 40:1) and stirring for 1h at 90°C, is possible to observe the color shift of the solution from brown to black,

that suggests a successful reduction (step 3). In the in-situ reduction procedure, the precipitation of RGO doesn't happen because HAVOH works as surfactant for RGO, stabilizing it in water. After reduction of GO, the solution is cooled at room temperature and HAVOH crosslinker is added to the solution (step 4). Then, the black solution is sprayed on PET substrate. Prepared solution is stable, even after 6 months.

Coating solutions based on HAVOH and RGO reduced by in-situ procedure contain high quantity of dehydroascorbic acid, that is the product of the reaction between L-ascorbic acid and graphene oxide. In not clear if dehydroascorbic acid can influence the water vapor barrier properties of the final coating.
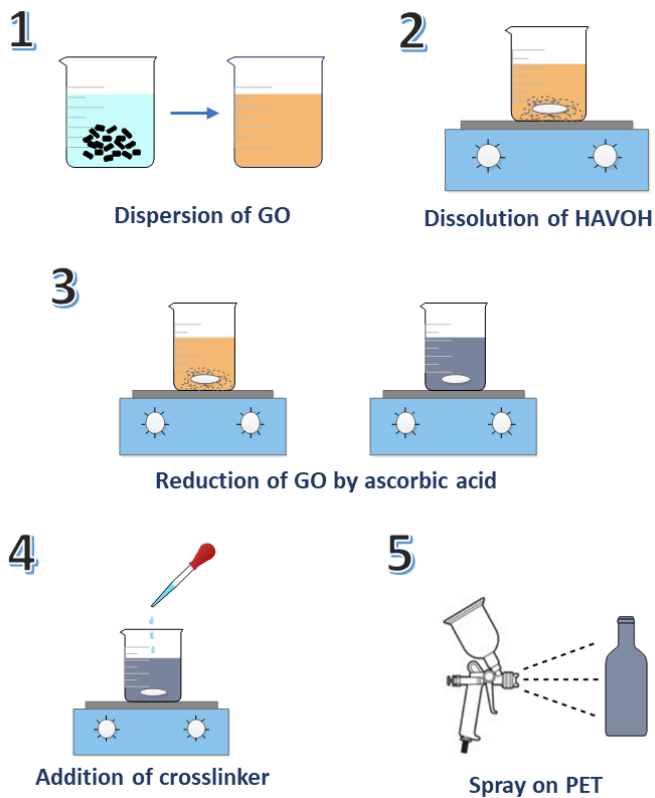
Figure 5.12 In-situ reduction procedure schematization.

5.4.3 Ex-situ reduction procedure

Reduced graphene oxide powder is not easy to disperse in aqueous solutions, due to the hydrophobic behavior of the powder. With the following procedure, is possible to obtain a reduced graphene oxide that can be dispersed in water solutions. The advantage of this procedure is to obtain a RGO free from dehydroascorbic acid, produced during the reduction by ascorbic acid.

The concept at the basis of the procedure is to wash the RGO powder with a HAVOH aqueous solution, in order to remove residual ascorbate and introduce the polymer as surfactant to stabilize the powder. HAVOH chains should intercalate between RGO sheets and increase the affinity with water solutions.

The procedure started from a commercial solution of graphene oxide. GO Punto Quantico is a stable water solution of 0.5%wt. In this commercial product, some surfactants are present to stabilize completely GO in water. The decision of start from the commercial product is attributable to the high concentration of GO in water, that allows to have a higher quantity of final product, compared with a lab GO aqueous solution.
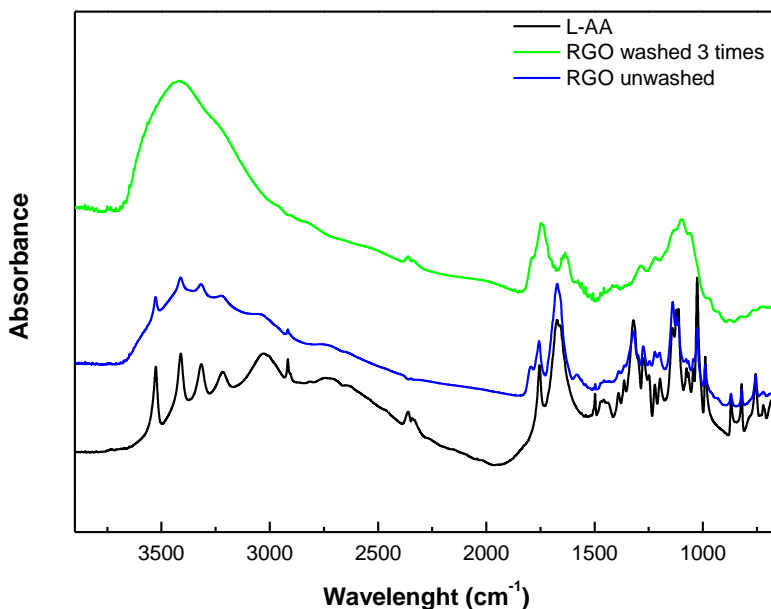
Figure 5.13 FTIR spectra for L-ascorbic acid, RGO unwashed and RGO washed three times.

L-Ascorbic acid (ratio 40:1 L-AA/GO) was added to commercial GO solution and the reduction was realized stirring at 90°C for 1h to achieve the shift of color and the precipitation of black powder that confirm the successful reduction of graphene oxide. The solution containing precipitated RGO was centrifuged at 9000 rpm for 15 min. After centrifugation, powder was recovered while supernatant was vacuum filtered, in order to recover as much powder as possible. All the powder recovered is washed with a HAVOH aqueous solution (5%wt). Then, the solution is centrifuged.

The operation of centrifugation, recovery of the powder and washing with HAVOH solution was repeated three times. The necessity of repeat three times this operation come from the fact that three washing steps are required to remove all the ascorbate from RGO, as demonstrated in FTIR spectra in figure 5.13. In fact, in RGO washed three times spectrum no traces of ascorbic acid are observed. The result of the last centrifugation is a masterbatch RGO/HAVOH. This masterbatch, illustrated in figure 5.14(a), can be easy dissolved in water by sonication, forming a stable RGO water solution, free from reduction products. A photographic image of purified RGO aqueous solution, realized sonicating RGO/HAVOH masterbatch in water, is reported in figure 5.14(b).

The limit of ex-situ reducing procedure is the low amount of masterbatch produced. In fact, for each centrifugation and filtration step, high amount of reduced graphene oxide is loss. Furthermore, the amount of reduced graphene oxide in the masterbatch is not well defined.
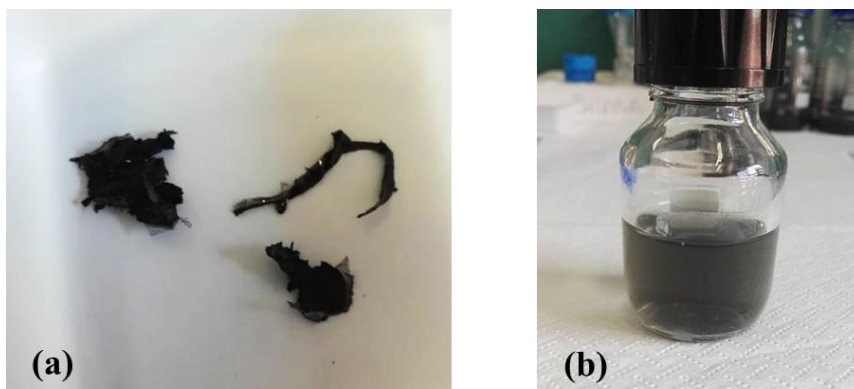
Figure 5.14 Photographic images of (a) RGO-HAVOH masterbatch and (b) water solution (0.1mg/ml) of masterbatch.

5.4.4 ██

████

██

██
██
██
██
██
██
██
██

███
██

██
██
██
██
██

███
███

██
███

5.4.5 ██
█████████████████████████
██
██
███

██
██

███
███
███
████████████████████████████████
███
███
████
███
███
███
███
███
███
███
███
███

███
███
███

███
███
███
██

5.4.6 RGO based coatings transparency

███
██

███
███

███
███
███
███
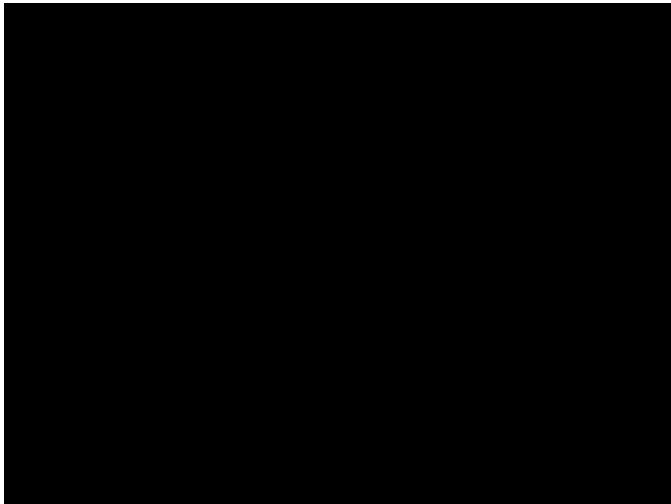
5. 5

Considerations and Future Developments

As demonstrated in this chapter, no further improvements were found using graphene-based as additives in developed coating. Reduced graphene oxide was found to be the most promising additive between the investigated ones, in term of possibility of further decrease WVTR of PET, and in term of industrial feasibility. Compared to graphene and graphene oxide, reduced graphene oxide represents a good compromise between high impermeability of graphene, due to its un-defective structure, and processability of graphene oxide, due to its high efficiency of dispersion in water solutions. In-situ reduction procedure is an easy method to produce stable RGO-HAVOH solutions, with high feasibility for high-scale processes. However, the grate limit in the use of RGO and, more in general, of graphene-based additives is their black color that influences negatively the coating transparency. This is a crucial point for the design of a coating for packaging applications, because black color coated bottles could be not sealable. In this case, an additional decorative coating should be applied, to avoid the negative impact on First Moment of Truth [Nelson and Ellison (2005)].

The aim of the use of graphene-based additives for developed coating was the achieving of the same result of water barrier obtained with 35 µm thick coating, with a thinner coating, because of increasing the tortuosity of the gas molecules path across the polymer matrix. The use of these additives should not influence negatively coating positive characteristics, such as transparency and wettability on PET. For these reasons, the use of 2D additives based on graphene to load barrier coating developed should be further investigated, to evaluate its benefits.

First, an investigation of the water barrier properties of RGO-loaded coatings should be implemented considering RGO content, compared to HAVOH, and dispersion in HAVOH. If RGO content is low, RGO sheets are far one from each other and gas molecules can pass easily between them. Hence, high RGO content is required to obtain the increase of the tortuosity of the gas molecules path across the matrix. However, high RGO content means high GO content in starting coating

solution. The dispersity of GO in water should be investigated, evaluating water barrier improvements, changing time and power of sonication of GO in water.

Another crucial point is the reduction of degree of RGO. In fact, high degree of reduction decreases the affinity between RGO and water vapor molecules, but the affinity between RGO and water solution is also decreased. This can cause the formation of aggregates of RGO that is not well dispersed in the solution. Hence, WVTR for RGO-loaded coatings should be investigated considering different degrees of reduction, in other words different concentration of ascorbic acid during GO reduction.

Compared to unloaded HAVOH solution, RGO-loaded solution is not easy to deposit by spray coating on PET substrates. Hence, a study of RGO solution wettability on PET should be run, considering eventually solvents to add to solution or pretreatments of PET surface that can improve wettability of RGO-loaded coating solutions on PET substrates.

CHAPTER

6

Application of developed coating matrix on real PET bottles

In this chapter, the developed water vapor barrier coating is applied on real PET bottles. Firstly, the Injection Stretch Blow Molding, that is the main technique for the large-scale production of PET bottle, is illustrated (§6.1). Then, an overview of the samples prepared is presented, defining the coating formula to deposit and spray parameters to consider (§6.2). The influence of the liquid/ air flow rate (§6.3) and of the drying rate (§6.4) on coating properties is considered. Furthermore, the phenomena that occur spraying successive layers are investigated (§6.5). Lastly, the possibility of combine the developed coating matrix with solvents that can improve the wettability of solution on PET is considered (§6.6).

Injection Stretch Blow molding for the realization of PET bottles

Blow molding is one of the most used techniques to produce a wide variety of hollow plastic parts such as bottles, drums, and tanks. Two main types of blow molding exist: extrusion blow molding and injection stretch blow molding. Extrusion blow molding involves the extrusion of a parison into a mold and its subsequent inflation to form the desired article [McEvoy et al. (1998)].

Injection stretch blow molding (ISBM) is one of the most popular blow-molding processes for making thin-walled PET bottles, achieving axial molecular orientation. This provides enhanced physical properties, such as high toughness, and gas barrier properties [Awaja and Pavel (2005)].
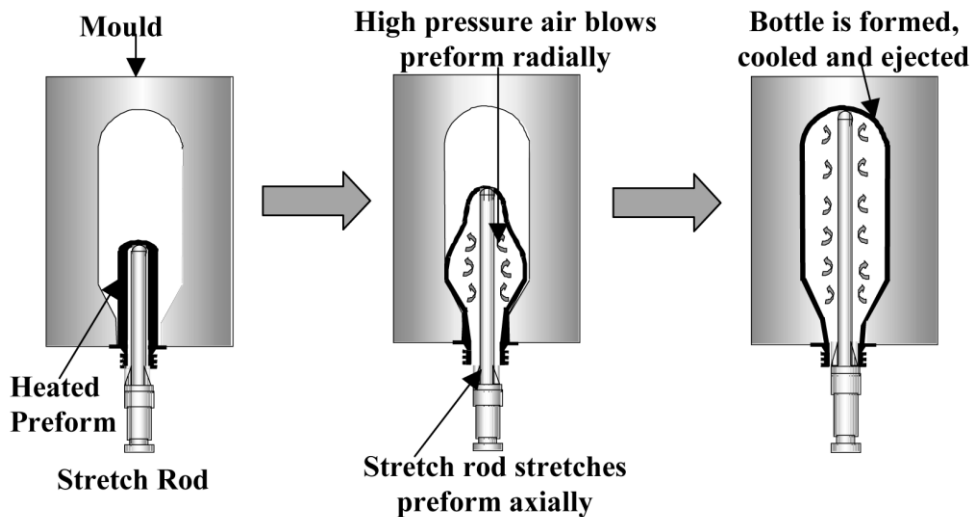
Figure 6.1 Schematic representation of Injection Stretch Blow Molding [Yang et al. (2014)].

Briefly, in ISBM process, the PET resin is first injected into a tube-shaped mold to make structurally amorphous preforms. The preforms are then heated in an

infrared oven above the glass transition temperature (typically T_g=80 °C), and then simultaneously stretched with a stretch rod and blown up with high-pressure air inside, to create bottles with desired shapes. The bottles are cooled in the mold and finally ejected. The whole deformation process is finished in a few seconds [Yang et al. (2004)]. There are two distinct stretch blow molding techniques: the one-stage process and two stage process.

In the one-stage process, the preform is injection molded, conditioned to the proper temperature and blown into a container, in one continuous process. The one-stage process is used in cases in which very high production rates are not required, as in the case of the production of wide-mouth jars. In the two-stage process, preforms are injection molded and stored. Then, are reheated by infrared heating elements, that produces a temperature profile along the length of the preform. The temperature profile causes a preferential stretching in the hotter regions. The heated preform, once properly conditioned, is positioned in the blow mold. The mold is then closed and a pre-blow is performed introducing low pressure air into the preform along with stretch rod motion. As the preform distorts, an aneurysm develops near the center of the side wall and at almost constant pressure, and the aneurysm spreads in both directions along the axis of the preform. Finally, after or near the end of the stretch rod motion, high-pressure air is introduced, completing the formation of the bottle. Because of the relatively high cost of the molding and equipment, this technique is best for producing high-volume items such as carbonated beverage bottles and detergent PET bottles [McEvoy et al. (1998)].

6. 2

Overview of coated PET bottles realization

██
██
██
██
████████████████████████████████
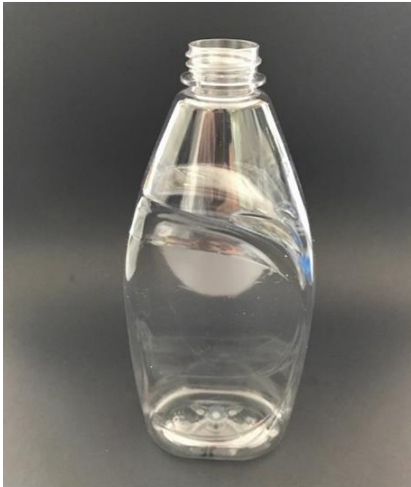
Figure 6.2 Photographic images of (a) PET bottle produced by LogoPlaste and (b) PET bottle commercialized by Procter & Gamble.

██
██
██
██
██
████████████████████████████████
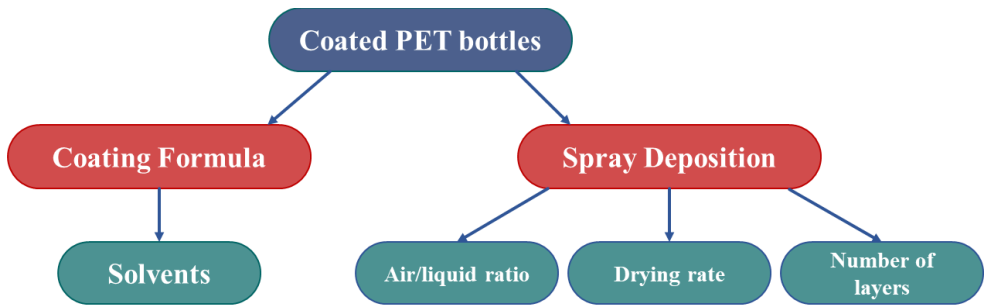
Figure 6.3 Overview of coated PET bottles prepared.

6. 3

Influence of air/liquid flow rate during spraying

As described in (§3.4), spray coating technique consists in the atomization of the liquid solution by an air source. The final product quality is highly influenced by the flow rate of liquid and air sprayed on the substrate. These parameters should be tailored according to the viscosity and the wettability of the solution.

Ideally, if high liquid flow rate is set up, the deposition of a high thickness coating on a large area results a fast operation. Nevertheless, spraying high quantity of liquid is possible only in the case in which the viscosity of the solution is high and/or the solution wettability on PET is good. Moreover, high liquid flow rate deposition can cause the formation of defects, called "sagging", on the final product surface. In fact, in the case of vertical surfaces, solution, that is not already dried, can flow on the surface, causing the formation of areas in which coating is accumulated.

Figure 6.4 Photographic image of "sagging" defect due to the high liquid flow rate [Source: Lechler].

Spray deposition with high air flow rate is ideal when the coating solution has low viscosity and/or when the wettability of the solution on PET is very low. In these cases, spraying low liquid quantity with high air flow rate helps the deposition

because the coating dries fast, due to the air. Furthermore, defects, such as sagging, are avoided. However, high air flow rate deposition results slow in the case of high thickness of the coating and large area of deposition. In fact, to achieve the desired thickness, successive layers are required.

To verify the influence of the flow rate on the quality of the final coated PET bottles, coated PET bottles were prepared spraying developed coating solution at different conditions: high liquid/low air flow rate, medium liquid/medium air flow rate, low liquid/high air flow rate. Coated bottles were then cut and analyzed with optical microscope in reflection mode, to observe the coating surface. In table 6.1, visual and touch appearance of the samples is reported.

Table 6.1 Visual and touch appearance of coated PET bottles varying liquid and air flow rate.

Flow Rate	Visual Appearance	Touch Appearance
High liquid/ low air	Glossy	Smooth
Medium liquid/ medium air	Glossy	Smooth
Low liquid/ high air	Mat	Rough

Coated PET bottle obtained spraying with high liquid/low air flow rate conditions appears glossy. The glossy coating appearance is confirmed by optical microscope image, as reported in figure 6.5 (b), that shows a uniform substrate with few defects.
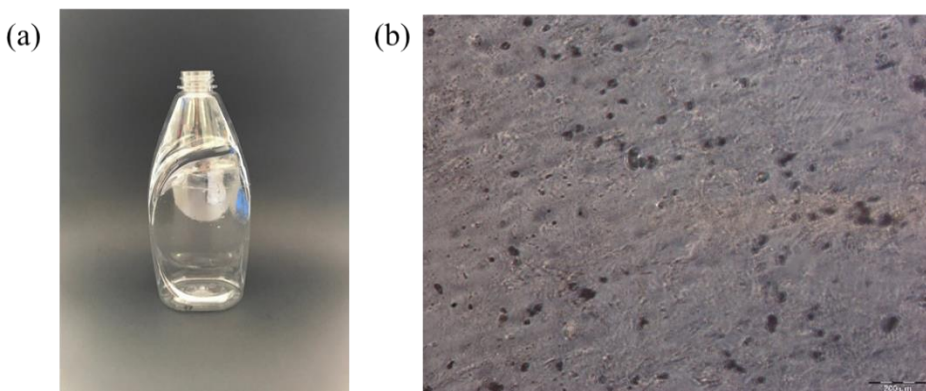
Figure 6.5 Photographic image (a) and optical microscope image (b) of PET bottle coated using high liquid/low air flow rate.

However, some "sagging" defects are observed on the surface, due to the low viscosity of the solution.
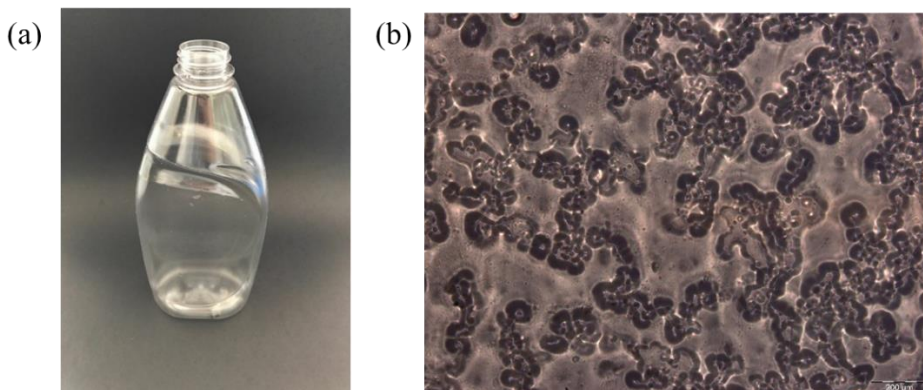
Figure 6.6 Photographic image (a) and optical microscope image (b) of PET bottle coated using low liquid/high air flow rate.

In the case in which PET bottle is coated spraying with low liquid/high air flow rate conditions, the sample appears mat. As is possible to observe in figure 6.6 (b), the mat appearance is attributable to a not uniform surface. In fact, the surface appears full of channel, that suggests a too fast evaporation of water. This situation is a common defect that can occurs when high air flow rate condition is used to spray a high drying coating.
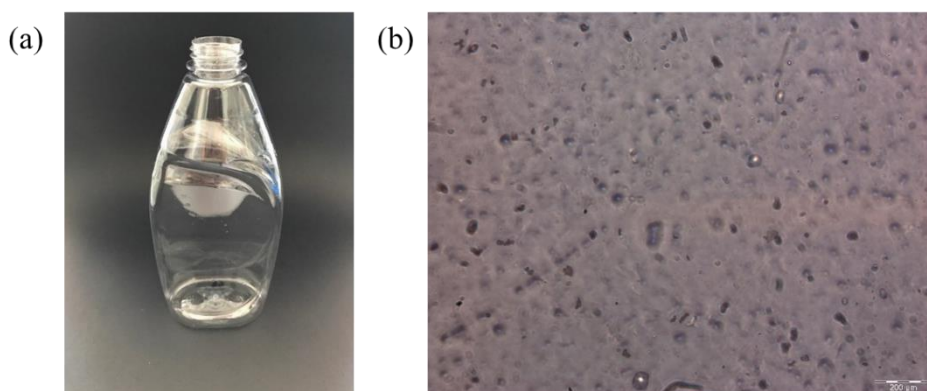
Figure 6.7 Photographic image (a) and optical microscope image (b) of PET bottle coated using medium liquid/medium air flow rate.

Coated PET bottle obtained spraying with medium liquid/medium air flow rate conditions appears glossy. As in the case of high liquid/low air flow rate conditions, the glossy coating appearance is confirmed by optical microscope image, as reported in figure 6.7 (b), that shows a uniform substrate with few defects. Furthermore, no macroscopic defects were observed. Hence, application of developed coating solution spraying with medium liquid/medium air flow rate conditions appears the best situation to obtain a high quality final product.

In figure 6.8, the transmittance at 550 nm [Lai et al. 2014] for coated bottles and uncoated one is reported, demonstrating the high transparency of samples prepared (transmittance over 85%).
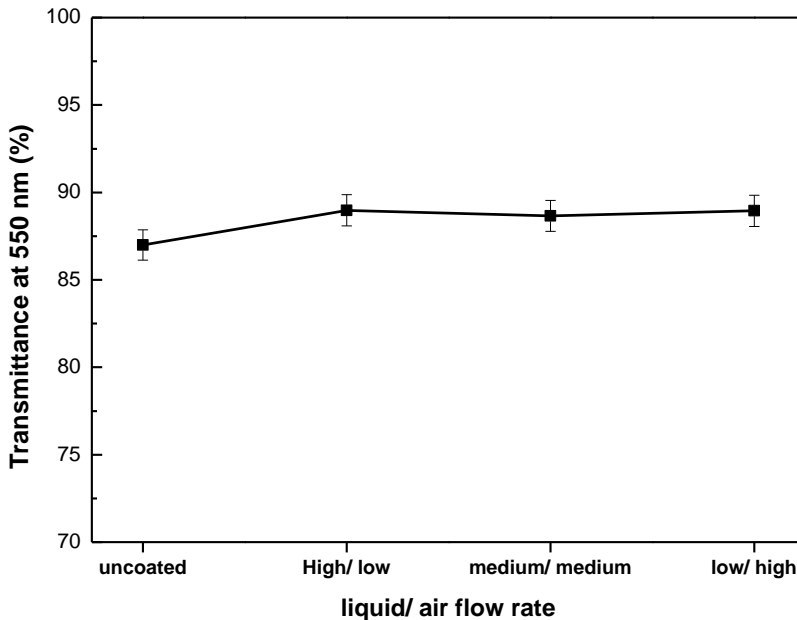
Figure 6.8 Transmittance at 550 nm for uncoated PET bottle and coated PET bottle sprayed varying liquid/air flow rate.

Influence of drying rate

During the industrial process, a forced drying is required, in order to achieve a as fast as possible deposition steps. However, a too fast drying can cause the formation of bobbles in the coating, affecting the appearance and properties of the coating. For these reason, the influence of drying rate should be investigated, to evaluate its influence on the appearance of the coated PET bottle.

The pilot plant chamber, usually employed for painted cars drying, in which samples were dried is illustrated in figure 6.9.
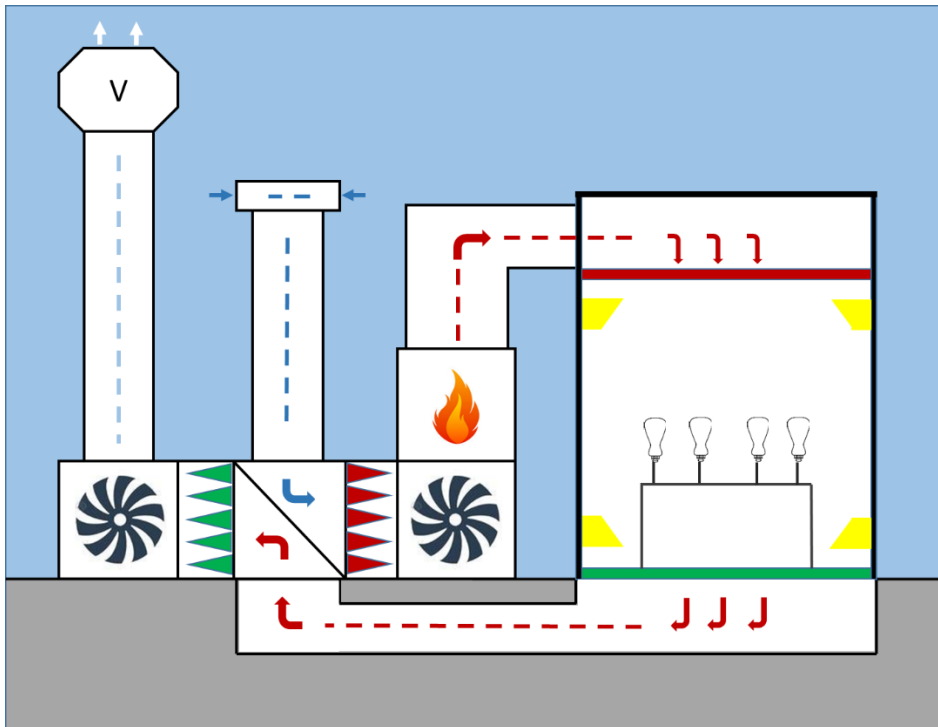
Figure 6.9 Schematic representation of pilot plant for PET bottle spray.

Air flows from up to down in the chamber at imposed temperature, and the drying rate can be automatically modulated ad "slow", "medium" and "fast". To evaluate

the influence of the drying rate on the coated PET bottles, was evaluated preparing coated PET bottles with the same liquid/air flow rate conditions (medium/medium) and dry them with two different air rates: medium and slow. In table 6.2 visual and touch appearance for prepared bottles is reported.

**Table 6.2** Visual and touch appearance of coated PET bottles varying drying rate.

Drying Rate	Visual Appearance	Touch Appearance
Slow	Glossy	Smooth
Medium	Pin holing	Rough

In case of slow drying rate set up, the coating appears glossy and uniform, as confirmed by photographic image in figure 6.10(a). The surface, reported in optical microscope image in figure 6.10(b), is highly homogeneous, with few defects.
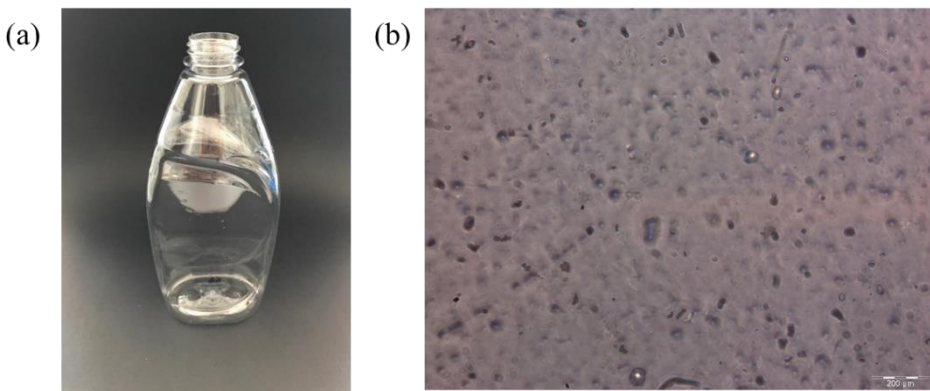
Figure 6.10 Photographic image (a) and optical microscope images (b) of coated PET bottle dried at medium rate.

Coated PET bottle dried at medium rate presents a highly not homogeneous surface, as demonstrated by optical microscope images in figure 6.10(b)(c). The bottle coating seems to be affected by the problematic of the "pin holing", that is a common defect that can occurs during drying. This defect, that consists in the formations of small deep holes in the coating, is attributable to the air trapped during the application of a high thickness coating. Due to high drying rate, air trapped in first layers leaves the coating too fast, forming small pinholes.

Pin holing highly affect the visual appearance of the final coated PET bottles, as shown in the photographic image in figure 6.11(a). For this reason, slow drying rate is required to obtain a glossy and smooth coating.
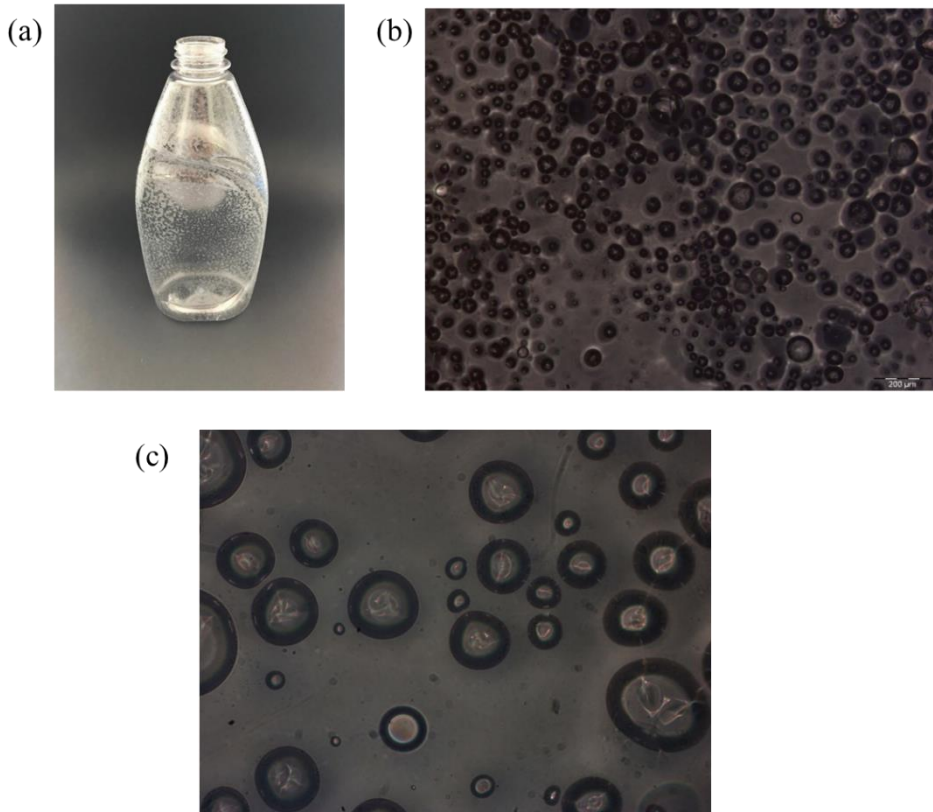
Figure 6.11 Photographic image (a) and optical microscope images at two magnifications(b) (c) of coated PET bottle dried at medium rate.

6. 5
Influence of number of layers deposited

Once established that medium liquid/ medium air flow rate is the best condition to spray the developed coating, is necessary to deposit successive layers to achieve thickness required for the water vapor barrier effect. However, deposition of successive layers delays the spray coating step and can cause the formation of defects.

To evaluate the influence of the number of layers deposited, coated PET bottles were sprayed in medium liquid/ medium air flow rate conditions and dried at slow air rate, varying the number of layer deposited: 1, 3, 5, 6.

In table 6.3 visual and touch appearance for prepared bottles is reported.

Table 6.3 Visual and touch appearance of coated PET bottles varying number of layers deposited.

Number of Layers	Visual Appearance	Touch Appearance
1 layer	Glossy	Smooth
3 layers	Glossy	Smooth
5 layers	Glossy	Smooth
6 layers	Cracking	Rough

Bottles coated one, three and five layers of coating solution appear glossy and uniformly coated, as illustrated in figure 6.12(a)(b)(c). Application of the sixth layer of coating causes the coating cracking, that is a phenomenon that can occurs for high thickness coatings. Water, evaporating from first layers deposited toward coating surface, induces stress in the coating that can crack. The result is an irregular breakup of the coating into small plates, still attached to the PET substrate.

The cracking of the coating can be macroscopically observed in figure 6.12(d), and a detail of a crack is reported by optical microscope image in figure 6.13(d).
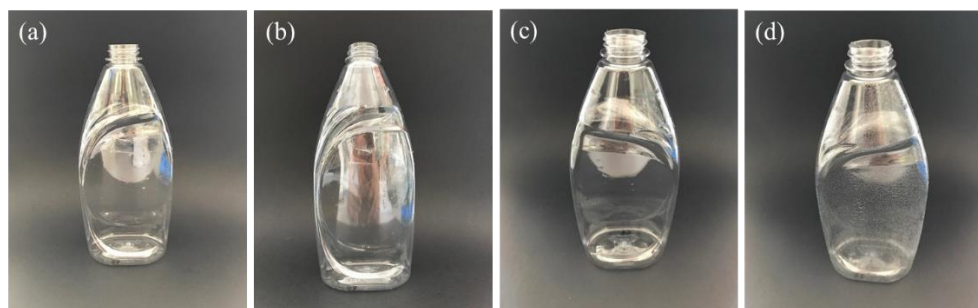
Figure 6.11 Photographic images of coated PET bottles with 1 layer (a), 3 layers (b), 5 layers (c), 6 layers (d).
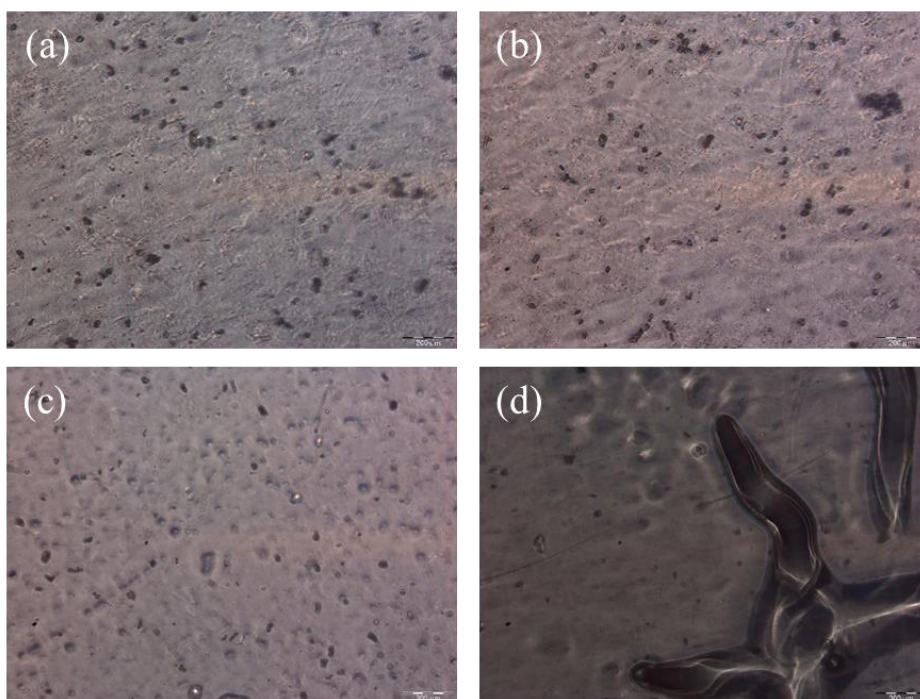
Figure 6.12 Optical microscope images
of coated PET bottles with 1 layer (a), 3 layers (b), 5 layers (c), 6 layers (d).

To achieve the thickness required for the water barrier effect reported in chapter 4, that is 35 µm, more than 6 layers are required. In fact, as reported in figure 6.13, coating cracking is associated to a hypothesized thickness of 25 µm. coating thicknesses were hypothesizing by weighting the bottles before and after spray

deposition. Cracking of the coating over 6 layers deposited could be avoided introducing solvents in the coating developed formula.
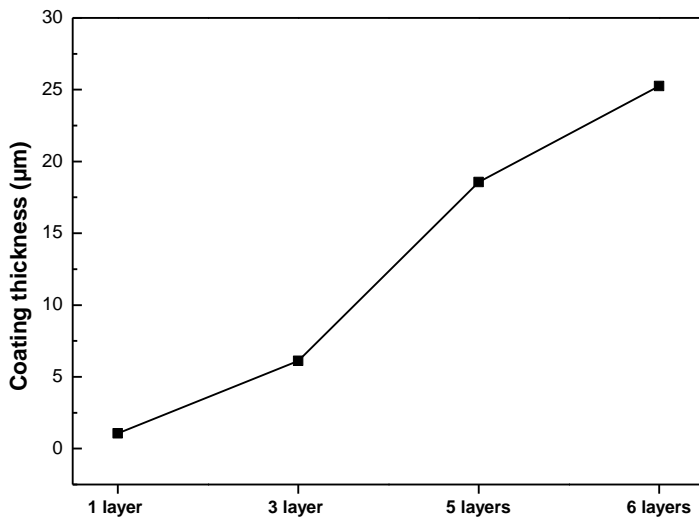
Figure 6.13 Hypothesized coating thickness for bottles sprayed with different number of layers.

6. 6
Solvents Evaluation

Coating formula showed two main problems during spray deposition: not optimal wettability on PET bottle, and fast evaporation of the water. These problematics limit the use of high liquid/ slow air flow rate conditions and a fast drying. Furthermore, over 25 µm of coating deposited, the coating cracking takes place. A possible solution could be the use of a solvent that improves the wettability of the solution on PET and retards the evaporation of water from the coating, without affecting the water vapor barrier effect.

Two different solvents were combined with coating formula developed: a dry retardant, and an anti-static agent. Dry retardant solvent is used for quick drying paints that can dry too fast, especially when the weather is hot or at very low humidity levels. Moreover, it is used in the case in which paint is based on toxic solvents, to reduce toxic fumes flow that comes out from the coating. Anti-static agent is a compound generally deposited on the surface before the application of a coating or on the final product, to reduce or eliminate static electricity. This reduces the accumulation of dust on the surface, avoiding eventual defects during the deposition of the coating. Anti-static further can be mixed with paint to improve the wettability of the paint on the substrate.

Developed coating formula was combined with dry retardant (30% vol) and deposited on a PET bottle using medium liquid/medium air flow rate conditions and slow drying. Same conditions were used to coat a PET bottle with developed coating formula combined with an anti-static agent (50% vol).

Table 6.4 Visual and touch appearance of coated PET bottles using different solvents.

Solvent	Visual Appearance	Touch Appearance
No solvent	Glossy	Smooth
Dry Retardant	Mat	Slightly Rough
Anti-static	Glossy	Smooth

In table 6.4, visual and touch appearance of prepared samples is reported and compared with a no coated PET bottle without solvent. Coating mixed with dry retardant has a mat slightly rough surface, as is possible to observe in the photographic image reported in figure 6.14(a). The rough surface is further demonstrated by the optical microscope image reported in figure 6.14(b), that shows a surface full of channels. This suggests that the use of the dry retardant indeed doesn't retard the drying of the water that forms channels across coating.
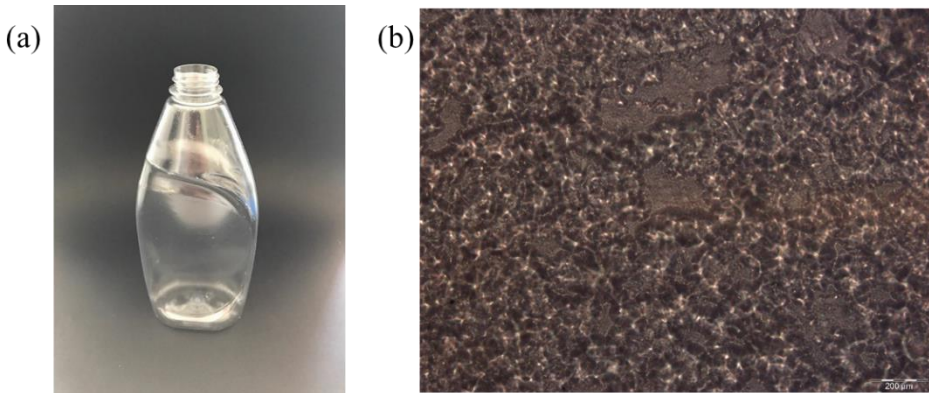
Figure 6.13 Photographic image (a) and optical microscope images (b) of PET bottle coated with developed coating mixed with dry retardant.
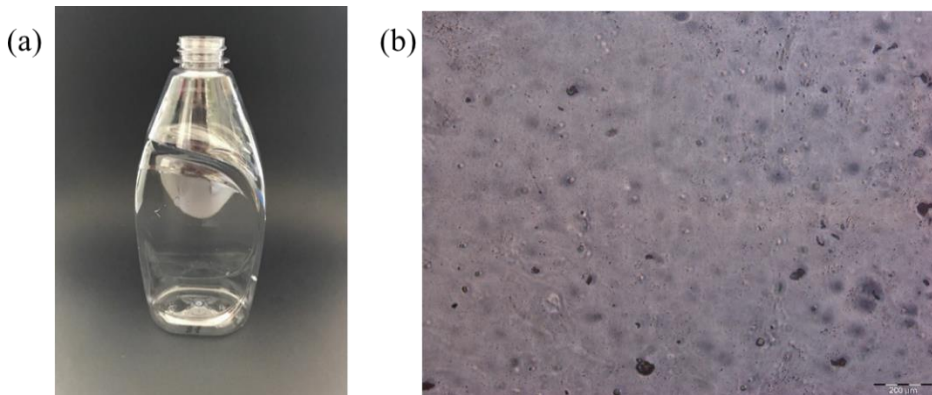
Figure 6.14 Photographic image (a) and optical microscope images (b) of PET bottle coated with developed coating mixed with anti-static agent.

Combining the developed coating solution with anti-static agent allows to a glossy and smooth coating. Furthermore, the wettability of the solution is improved during the spraying, that results easier and faster.

Visual appearance of the coating is confirmed by UV-vis analysis. As reported in figure 6.15, the transmittance at 550 nm confirms the transparency of the coated PET bottles (transmittance >85%), even if in the case of use of the dry retardant the transmittance value is lower, compared to other samples.
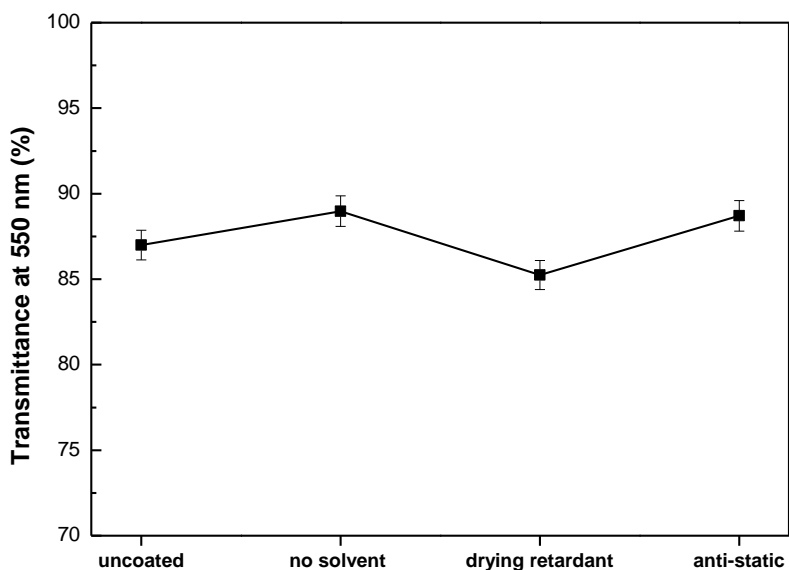
Figure 6.15 Photographic image (a) and optical microscope images (b) of PET bottle coated with developed coating mixed with dry retardant.

6.7
Future Developments

Conclusions

Plastic materials are ideal for packaging application, due to unique characteristics, such as transparency and lightness. Among polymers, Polyethylene Terephthalate is one of the most used polymer in packaging applications, especially in bottles for carbonated drinks. The limit of the use of polymers in packaging is their low barrier to gases, water vapor and flavors with a negative impact on the quality of the product. Although gas and flavors barrier technologies are already implemented on large-scale, water vapor barrier technologies are still in design stage.

Possible technological routes should be amenable to an industrial implementation, sustainable and with no impact on bottle appearance. Coating technology can satisfy all the requirements for the industrial implementation, because high performances can be achieved adding a thin barrier material, minimizing the negative impact on the recycling process. Among all the coating deposition techniques, spray coating is the most feasible for large-scale implementation. For example, spray coating is the main technique for paint deposition in automotive.

The concept of the dissertation was the design of a water vapor coating to apply by spray coating on PET containers. The coating could be composed by a barrier matrix eventually loaded with 2D- additives to further increase water vapor barrier effect. Once designed coating, the implementation on real bottles was performed, establishing spray coating parameters to obtain a high-quality coating.

The design of the coating started from the choice of the polymer to modify. HAVOH, that is a high amorphous vinyl alcohol polymer, was chosen as starting point for the coating design. This polymer, that is a derivate of PVA, has high oxygen barrier properties and is easy to use as coating. Furthermore, it is transparent and biodegradable. However, its amorphous morphology makes HAVOH easy to disperse in water, due to its high solubility. His affinity with water gives low water vapor barrier properties to HAVOH. To modify HAVOH and to achieve water vapor barrier, chemical crosslinking was chosen as strategy.

████████████ WVTR tests performed in two different configurations of the coated film demonstrated that is more convenient to apply coating outside the bottle. In fact, compared to the case in which the coating is applied inside the bottle, average humidity in which coating works is lower and this configuration results more favorable. To evaluate the industrial feasibility of this developed formulation, recycling protocol was applied to coated PET demonstrating that coating can be easy removed by PET, under conditions provided by recycling protocol.

████████ Graphene-based additives (graphene, graphene oxide, reduced graphene oxide) are considered as possible additives for the developed coating. They are widely used in literature to improve gas barrier properties of a polymer matrix. In fact, 2D-impermeable additives, such as graphene-based ones, reduce gas solubility, due to insolubility of gas in the nanosheets, and diffusivity, as the gas molecules must move around the impermeable nanosheets to diffuse through the polymer.

WVTR and OTR tests were performed to evaluate the effective ability of graphene-based additives to further improve water vapor barrier properties of crosslinked HAVOH coatings. Results performed on graphene-loaded coatings on PET films demonstrated that the inefficient dispersion of graphene in HAVOH causes an increase of both WVTR and OTR. In the case of graphene oxide-loaded coatings, the presence of additives caused a decrement of OTR and an increase of WVTR, compared to unloaded coatings. This result was expected because, even if

oxygen functionalities present on basal planes of GO guarantee an efficient dispersion in polymer matrix, they interact with water molecules, due to their hydrophilic behavior. Hence, the passage of oxygen molecules across the polymer matrix is obstructed by graphene oxide, while the passage of water molecules is simplified by the interaction between water and oxygen functionalities of GO basal planes. These oxygen functionalities can be removed using in a reducing chemical agent. Ascorbic acid was chosen as reducing agent for GO, due to its reduction efficiency and non-toxicity. The quantity of ascorbic acid required for high reduction of GO (40 mg of ascorbic acid each mg of GO) was evaluated considering color shift and quantity of RGO precipitated.

Two procedures of reduction were developed: one in which reduction occurs in the coating solution (in-situ procedure), and one in which RGO is reduced and then dispersed in coating solution (ex-situ procedure). ██████████████████ ██ ███ █████████████████████ RGO seems to be the promising additive for crosslinked HAVOH matrix. However, some parameters should be further investigated, such as dispersion efficiency of additives and RGO degree of reduction. In fact, even if reduction guarantees the change of behavior from hydrophilic to hydrophobic, suppression of all oxygen functionalities of GO decreases the dispersion efficiency of the additives.

████████████████████ coating was sprayed on real PET bottles, to evaluate optimal spray coating conditions. Three parameters were considered: liquid/air flow rate, drying rate, and number of layers deposited. Medium liquid/medium air flow rate and slow drying rate are required to obtain a glossy and smooth coating surface. Over six layers, coating cracking occurs. To prevent the formation of defects, such as cracking, the possibility of mix coating solution with other solvents was considered. It was demonstrated that, in terms of quality of coating and wettability of coating solution on PET, the combination of developed coating formula with an anti-static solvent was the best combination. Anti-static solvent increases the wettability of developed solution on PET and retards water drying, causing the formation of a compact and glossy coating with high thickness. Influence of anti-static solvent on water vapor barrier properties of developed coating was already not investigated. The PhD work demonstrated that coating formula developed is promising for industrial application, due to its chemical properties (water vapor and oxygen barrier, transparency) combined with industrial feasibility (ease to coating, no thermal treatment needed, recyclability).

Materials & Characterization

In this section all the experimental details have been collected. The selected raw materials are listed. Then, the processing conditions used for the preparation of the polymer nanocomposites are reported. The exploited characterization methods and the testing conditions are finally specified.

Raw materials

Chemicals used for the realization of water vapor coatings are:

(i) Water soluble HAVOH (G-Polymer OKS-8049) were purchased from Nippon Gohsei.

(ii) ███
███████

(iii) ██

(iv) ██
██████

(v) ██
██████

(vi) ████████████████████████████████████

(vii) L-Ascorbic acid was purchased from Sigma Aldrich;

(viii) GO was synthesized from purified natural graphite according to Hummers' method [Hummers and Offeman (1958)].

(ix) Dry retardant solvent (Glasurit 93-E3 Adjusting Base Slow) was supplied by BASF.

(x) Anti-static solvent (Glasurit 700-1 Cleaner) was supplied by BASF.

Substrates used for coating deposition are:

(i) Corona-treated Poly Ethylene Terephthalate, (PXEH) films with a thickness of 30 µm were supplied by Nuroll spa (Italy).;

(ii) PET Mars bottles (450 ml) were supplied by LogoPlaste.

For the sake of clarity, each material is related to the corresponding Chapter(s) in Table M&C.1

Table M&C .1 Selected raw materials, both chemicals and substrates, and corresponding Chapter(s).

	Materials	**Chapter(s)**
CHEMICALS	HAVOH	4, 5, 6
	███████████████	4, 5
	██████	4
	█████████	4
	█████████	4, 5, 6
	███████	4, 5, 6
	L-Ascorbic Acid	4, 5
	Graphene oxide	4, 5
	Dry retardant	6
	Anti-static	6
SUBSTRATES	PET film	4, 5
	PET bottle	6

Characterization methods

Characterization methods performed during the dissertation are:

(i) The oxygen transmission rate was measured using a standard permeabilimeter (Extrasolution, MULTIPERM), at 27°C and 0%, 50%, 70%, 90%, 100% RH.

(ii) The water vapor transmission rate was measured using a standard permeabilimeter (Extrasolution, MULTIPERM), at 25°C and 0%, 50%, 70%, 90% RH.

(iii) FTIR analysis were carried out in ATR mode with a Perkin Elmer Spectrum One FTIR spectrometer at a resolution of 4 cm^{-1} and 32 scan collections between 4000 and 650 cm^{-1}.

(iv) UV-Vis analysis were carried out in Transmittance mode with a Agilent Cary 60 UV spectrometer between 700 and 390 nm.

(v) Optical microscopy was performed by Olympus BX 51M.

For the sake of clarity, each characterization method is related to the corresponding Chapter(s) in Table M&C.2.

Table M&C .2 Characterization methods and corresponding Chapter(s).

Methods	Chapter(s)
OTR test	4, 5,
WVTR test	4, 5
FTIR analysis	4,5
UV analysis	4,5,6
Optical microscopy	6

References

Arora, A., & Padua, G. W. (2010). Nanocomposites in food packaging. *Journal of Food science*, *75(1).*

Ashley, R. J. (1985). Permeability and plastics packaging. In Polymer permeability (pp. 269-308). Springer Netherlands.

Awaja, F., & Pavel, D. (2005). Recycling of PET. *European Polymer Journal*, *41(7),* 1453-1477.

Balandin, A. A., Ghosh, S., Bao, W., Calizo, I., Teweldebrhan, D., Miao, F., & Lau, C. N. (2008). Superior thermal conductivity of single-layer graphene. *Nano letters*, *8(3),* 902-907.

Becerril, H. A., Mao, J., Liu, Z., Stoltenberg, R. M., Bao, Z., & Chen, Y. (2008). Evaluation of solution-processed reduced graphene oxide films as transparent conductors. *ACS nano*, *2(3)*, 463-470.

Berlinet, C., Brat, P., & Ducruet, V. (2008). Quality of orange juice in barrier packaging material. *Packaging Technology and Science*, *21(5)*, 279-286.

Berger, C., Song, Z., Li, X., Wu, X., Brown, N., Naud, C., ... & Conrad, E. H. (2006). Electronic confinement and coherence in patterned epitaxial graphene. *Science*, *312*(5777), 1191-1196.

Birck, C., Degoutin, S., Tabary, N., Miri, V., & Bacquet, M. (2014). New crosslinked cast films based on poly (vinyl alcohol): Preparation and physico-chemical properties. *Express Polymer Letters*, *8*(12).

Bolotin, K. I., Sikes, K. J., Jiang, Z., Klima, M., Fudenberg, G., Hone, J., ... & Stormer, H. L. (2008). Ultrahigh electron mobility in suspended graphene. *Solid State Communications*, *146*(9), 351-355.

Bolto, B., Tran, T., Hoang, M., & Xie, Z. (2009). Crosslinked poly (vinyl alcohol) membranes. *Progress in Polymer Science*, *34*(9), 969-981.

Campbell-Platt, G. (2017). *Food science and technology*. John Wiley & Sons.

Chen, C. T., Chang, Y. J., Chen, M. C., & Tobolsky, A. V. (1973). Formalized poly (vinyl alcohol) membranes for reverse osmosis. *Journal of Applied Polymer Science*, *17*(3), 789-796.

Chen, W., Yan, L., & Bangal, P. R. (2010). Preparation of graphene by the rapid and mild thermal reduction of graphene oxide induced by microwaves. *Carbon*, *48*(4), 1146-1152.

Choudalakis, G., & Gotsis, A. D. (2009). Permeability of polymer/clay nanocomposites: a review. *European polymer journal*, *45*(4), 967-984.

Compton, O. C., Kim, S., Pierre, C., Torkelson, J. M., & Nguyen, S. T. (2010). Crumpled graphene nanosheets as highly effective barrier property enhancers. *Advanced materials*, *22*(42), 4759-4763.

Deilmann, M., Halfmann, H., Steves, S., Bibinov, N., & Awakowicz, P. (2009). Silicon oxide permeation barrier coating and plasma sterilization of PET bottles and foils. *Plasma Processes and Polymers*, *6*(S1).

Demazeau, G. (1999). Solvothermal processes: a route to the stabilization of new materials. *Journal of Materials Chemistry*, *9*(1), 15-18.

Donato, K. Z., Lavorgna, M., Donato, R. K., Raucci, M. G., Buonocore, G. G., Ambrosio, L., ... & Mauler, R. S. (2016). High Amorphous Vinyl Alcohol-Silica Bionanocomposites: Tuning Interface Interactions with Ionic Liquids. *ACS Sustainable Chemistry & Engineering*, *5*(1), 1094-1105.

Eizenberg, M., & Blakely, J. M. (1979). Carbon monolayer phase condensation on Ni (111). *Surface Science*, *82*(1), 228-236.

Fernández-Merino, M. J., Guardia, L., Paredes, J. I., Villar-Rodil, S., Solís-Fernández, P., Martínez-Alonso, A., & Tascon, J. M. D. (2010). Vitamin C is an ideal substitute for hydrazine in the reduction of graphene oxide suspensions. *The Journal of Physical Chemistry C*, *114*(14), 6426-6432.

Ferrari, A. C., Bonaccorso, F., Fal'Ko, V., Novoselov, K. S., Roche, S., Bøggild, P., ... & Garrido, J. A. (2015). Science and technology roadmap for graphene, related two-dimensional crystals, and hybrid systems. *Nanoscale*, *7*(11), 4598-4810.

Gao, J., Liu, F., Liu, Y., Ma, N., Wang, Z., & Zhang, X. (2010). Environment-friendly method to produce graphene that employs vitamin C and amino acid. *Chemistry of Materials*, *22*(7), 2213-2218.

Gao, Y., Ye, H., Wang, L., & Liu, M. (2017). Experimental investigation of the effects of crosslinking processes on the swelling and hygroscopic performances of a poly (vinyl alcohol) membrane. *Journal of Applied Polymer Science*, *134*(7).

Geim, A. K., & Novoselov, K. S. (2007). The rise of graphene. *Nature materials*, *6*(3), 183-191.

Girotto, C., Rand, B. P., Genoe, J., & Heremans, P. (2009). Exploring spray coating as a deposition technique for the fabrication of solution-processed solar cells. *Solar energy materials and solar cells*, *93*(4), 454-458.

Gómez-Navarro, C., Weitz, R. T., Bittner, A. M., Scolari, M., Mews, A., Burghard, M., & Kern, K. (2007). Electronic transport properties of individual chemically reduced graphene oxide sheets. *Nano letters*, *7*(11), 3499-3503.

He, H., Klinowski, J., Forster, M., & Lerf, A. (1998). A new structural model for graphite oxide. *Chemical physics letters*, *287*(1), 53-56.

Hernandez, R. J. (1997). Food packaging materials, barrier properties and selection. *Handbook of Food Engineering Practice*.

Hummers Jr, W. S., & Offeman, R. E. (1958). Preparation of graphitic oxide. *Journal of the American Chemical Society*, *80*(6), 1339-1339.

Jiang, J. W., Wang, J. S., & Li, B. (2009). Young's modulus of graphene: a molecular dynamics study. *Physical Review B*, *80*(11), 113405.

Jiao, L., Zhang, L., Wang, X., Diankov, G., & Dai, H. (2009). Narrow graphene nanoribbons from carbon nanotubes. *Nature*, *458*(7240), 877.

Katz, M. G., & Wydeven, T. (1981). Selective permeability of PVA membranes. I. Radiation-crosslinked membranes. *Journal of Applied Polymer Science*, *26*(9), 2935-2946.

Kim, H. M., Lee, J. K., & Lee, H. S. (2011). Transparent and high gas barrier films based on poly (vinyl alcohol)/graphene oxide composites. *Thin Solid Films*, *519*(22), 7766-7771.

Kim, H., & Macosko, C. W. (2009). Processing-property relationships of polycarbonate/graphene composites. *Polymer*, *50*(15), 3797-3809.

Kumar, A., & Han, S. S. (2017). PVA-based hydrogels for tissue engineering: A review. *International Journal of Polymeric Materials and Polymeric Biomaterials*, *66*(4), 159-182.

Lai, C. L., Chen, J. T., Fu, Y. J., Liu, W. R., Zhong, Y. R., Huang, S. H., ... & Lee, K. R. (2015). Bio-inspired cross-linking with borate for enhancing gas-barrier properties of poly (vinyl alcohol)/graphene oxide composite films. *Carbon*, *82*, 513-522.

Lange, J., & Wyser, Y. (2003). Recent innovations in barrier technologies for plastic packaging—a review. *Packaging Technology and Science*, *16*(4), 149-158.

Layek, R. K., Das, A. K., Park, M. U., Kim, N. H., & Lee, J. H. (2014). Layer-structured graphene oxide/polyvinyl alcohol nanocomposites: dramatic enhancement of hydrogen gas barrier properties. *Journal of Materials Chemistry A*, *2*(31), 12158-12161.

Lee, P. J., Ho, C. C., Hwang, C. S., & Ding, S. J. (2014). Improved physicochemical properties and biocompatibility of stainless steel implants by PVA/ZrO 2-based composite coatings. *Surface and Coatings Technology*, *258*, 374-380.

Leenaerts, O., Partoens, B., & Peeters, F. M. (2008). Graphene: A perfect nanoballoon. *Applied Physics Letters*, *93*(19), 193107.

Lerf, A., He, H., Forster, M., & Klinowski, J. (1998). Structure of graphite oxide revisited‖. *The Journal of Physical Chemistry B*, *102*(23), 4477-4482.

Lim, M., Kim, D., & Seo, J. (2016). Enhanced oxygen-barrier and water-resistance properties of poly (vinyl alcohol) blended with poly (acrylic acid) for packaging applications. *Polymer International*, *65*(4), 400-406.

Loryuenyong, V., Saewong, C., Aranchaiya, C., & Buasri, A. (2015). The improvement in mechanical and barrier properties of poly (vinyl alcohol)/graphene oxide packaging films. *Packaging Technology and Science*, *28*(11), 939-947.

Mancini, S. D., & Zanin, M. (2000). Consecutive steps of PET recycling by injection: evaluation of the procedure and of the mechanical properties. *Journal of Applied Polymer Science*, *76*(2), 266-275.

Mansur, H. S., Sadahira, C. M., Souza, A. N., & Mansur, A. A. (2008). FTIR spectroscopy characterization of poly (vinyl alcohol) hydrogel with different hydrolysis degree and chemically crosslinked with glutaraldehyde. *Materials Science and Engineering: C*, *28*(4), 539-548.

Marin, E., & Rojas, J. (2015). Evaluation of crosslinking on the water sorption properties of poly (vinyl) alcohol. *Int. J. Pharm. Sci. Rev. Res*, *35*, 189.

Mathlouthi, M. (2013). *Food packaging and preservation*. Springer Science & Business Media.

McAllister, M. J., Li, J. L., Adamson, D. H., Schniepp, H. C., Abdala, A. A., Liu, J., ... & Aksay, I. A. (2007). Single sheet functionalized graphene by oxidation and thermal expansion of graphite. *Chemistry of materials*, *19*(18), 4396-4404.

McBride, J. S., Massaro, T. A., & Cooper, S. L. (1979). Diffusion of gases through polyurethane block polymers. *Journal of Applied Polymer Science*, *23*(1), 201-214.

McEvoy, J. P., Armstrong, C. G., & Crawford, R. J. (1998). Simulation of the stretch blow molding process of PET bottles. *Advances in Polymer Technology*, *17*(4), 339-352.

Mohanty, N., Nagaraja, A., Armesto, J., & Berry, V. (2010). High-throughput, ultrafast synthesis of solution-dispersed graphene via a facile hydride chemistry. *Small*, *6*(2), 226-231.

Moon, I. K., Lee, J., Ruoff, R. S., & Lee, H. (2010). Reduced graphene oxide by chemical graphitization. *Nature communications*, *1*(6), 73.

Nakaya, M., Uedono, A., & Hotta, A. (2015). Recent progress in gas barrier thin film coatings on pet bottles in food and beverage applications. *Coatings*, *5*(4), 987-1001.

Nelson, E. & Ellison, S. (2005). In a Shift, Marketers Beef Up Ad Spending Inside Stores. *The Wall Street Journal.*

Nicolosi, V., Chhowalla, M., Kanatzidis, M. G., Strano, M. S., & Coleman, J. N. (2013). Liquid exfoliation of layered materials. *Science*, *340*(6139), 1226419.

Nielsen, L. E. (1967). Models for the permeability of filled polymer systems. *Journal of Macromolecular Science—Chemistry*, *1*(5), 929-942.

Novoselov, K. S., Geim, A. K., Morozov, S. V., Jiang, D., Zhang, Y., Dubonos, S. V., ... & Firsov, A. A. (2004). Electric field effect in atomically thin carbon films. *science*, *306*(5696), 666-669.

Ofstead, R. F., & Poser, C. I. (1989). Semicrystalline poly (vinyl alcohol) hydrogels. *Advances in Chemistry,* 4, 61–72.

Paolilli, T. & Fitch, J. (2016). Barrier coating composition with organic particles EP 2625225 B1.

Paton, K. R., Varrla, E., Backes, C., Smith, R. J., Khan, U., O'Neill, A., ... & Higgins, T. (2014). Scalable production of large quantities of defect-free few-layer graphene by shear exfoliation in liquids. *Nature materials*, *13*(6), 624-630.

Pei, S., & Cheng, H. M. (2012). The reduction of graphene oxide. *Carbon*, *50*(9), 3210-3228.

Prasad, S. G., De, A., & De, U. (2011). Structural and optical investigations of radiation damage in transparent PET polymer films. *International Journal of Spectroscopy*, *2011*.

Pu, N. W., Wang, C. A., Liu, Y. M., Sung, Y., Wang, D. S., & Ger, M. D. (2012). Dispersion of graphene in aqueous solutions with different types of surfactants and the production of graphene films by spray or drop coating. *Journal of the Taiwan Institute of Chemical Engineers*, *43*(1), 140-146.

Robertson, G. L. (2016). *Food packaging: principles and practice*. CRC press.

Schniepp, H. C., Li, J. L., McAllister, M. J., Sai, H., Herrera-Alonso, M., Adamson, D. H., ... & Aksay, I. A. (2006). Functionalized single graphene sheets derived from splitting graphite oxide. *The Journal of Physical Chemistry B*, *110*(17), 8535-8539.

Seethamraju, S., Kumar, S., Madras, G., Raghavan, S., & Ramamurthy, P. C. (2016). Million-Fold Decrease in Polymer Moisture Permeability by a Graphene Monolayer. *ACS nano*, *10*(7), 6501-6509.

Simon, D. A., Bischoff, E., Buonocore, G. G., Cerruti, P., Raucci, M. G., Xia, H., ... & Mauler, R. S. (2017). Graphene-based masterbatch obtained via modified polyvinyl alcohol liquid-shear exfoliation and its application in enhanced polymer composites. *Materials & Design*, *134*, 103-110.

Shirakura, A., Nakaya, M., Koga, Y., Kodama, H., Hasebe, T., & Suzuki, T. (2006). Diamond-like carbon films for PET bottles and medical applications. *Thin Solid Films*, *494*(1), 84-91.

Sreedhar, B., Sairam, M., Chattopadhyay, D. K., Rathnam, P. A., & Rao, D. V. (2005). Thermal, mechanical, and surface characterization of starch–poly (vinyl alcohol) blends and borax-crosslinked films. *Journal of Applied Polymer Science*, *96*(4), 1313-1322.

Stankovich, S., Dikin, D. A., Piner, R. D., Kohlhaas, K. A., Kleinhammes, A., Jia, Y., ... & Ruoff, R. S. (2007). Synthesis of graphene-based nanosheets via chemical reduction of exfoliated graphite oxide. *carbon*, *45*(7), 1558-1565.

Stone, S. A., Gosavi, P., Athauda, T. J., & Ozer, R. R. (2013). In situ citric acid crosslinking of alginate/polyvinyl alcohol electrospun nanofibers. *Materials Letters*, *112*, 32-35.

Su, Y., Kravets, V. G., Wong, S. L., Waters, J., Geim, A. K., & Nair, R. R. (2014). Impermeable barrier films and protective coatings based on reduced graphene oxide. *arXiv preprint arXiv:1405.2360*.

Thomas, L. V., Arun, U., Remya, S., & Nair, P. D. (2009). A biodegradable and biocompatible PVA–citric acid polyester with potential applications as matrix for vascular tissue engineering. *Journal of Materials Science: Materials in Medicine*, *20*(1), 259.

Tracton, A. A. (Ed.). (2006). Coatings technology: fundamentals, testing, and processing techniques. *CRC Press*.

Valentas, K. J., Rotstein, E., & Singh, R. P. (1997). *Handbook of food engineering practice*. CRC press.

Wang, J., Liang, M., Fang, Y., Qiu, T., Zhang, J., & Zhi, L. (2012). Rod-coating: towards large-area fabrication of uniform reduced graphene oxide films for flexible touch screens. *Advanced Materials*, *24*(21), 2874-2878.

Wang, X., Zhi, L., & Müllen, K. (2008). Transparent, conductive graphene electrodes for dye-sensitized solar cells. *Nano letters*, *8*(1), 323-327.

Witte, D.H. (2003). Proceedings of Nova-Pack Europe 2003, Munich, p. 39.

Wolf, R., Wandel, K., & Boeffel, C. (2007). Moisture Barrier Films Deposited on PET by ICPECVD of SiNx. *Plasma Processes and Polymers*, *4*(S1).

Wu, T., Liu, S., Li, H., Wang, L., & Sun, X. (2011). Production of reduced graphene oxide by UV irradiation. *Journal of nanoscience and nanotechnology*, *11*(11), 10078-10081.

Wu, Z. S., Ren, W., Gao, L., Liu, B., Jiang, C., & Cheng, H. M. (2009). Synthesis of high-quality graphene with a pre-determined number of layers. *Carbon*, *47*(2), 493-499.

Xianda, Y., Anlai, W., & Suqin, C. (1987). Water-vapor permeability of polyvinyl alcohol films. *Desalination*, *62*, 293-297.

Yan, N., Buonocore, G., Lavorgna, M., Kaciulis, S., Balijepalli, S. K., Zhan, Y., ... & Ambrosio, L. (2014). The role of reduced graphene oxide on chemical, mechanical and barrier properties of natural rubber composites. *Composites Science and Technology*, *102*, 74-81.

Yan, N., Capezzuto, F., Buonocore, G. G., Lavorgna, M., Xia, H., & Ambrosio, L. (2015). Gas-barrier hybrid coatings by the assembly of novel poly (vinyl alcohol) and reduced graphene oxide layers through cross-linking with zirconium adducts. *ACS applied materials & interfaces*, *7*(40), 22678-22685.

Yan, X. T., & Xu, Y. (2010). Chemical vapour deposition: an integrated engineering design for advanced materials. *Springer Science & Business Media*.

Yang, Y. H., Bolling, L., Priolo, M. A., & Grunlan, J. C. (2013). Super gas barrier and selectivity of graphene oxide-polymer multilayer thin films. *Advanced Materials*, *25*(4), 503-508.

Yang, Z. J., Harkin-Jones, E., Menary, G. H., & Armstrong, C. G. (2004). A non-isothermal finite element model for injection stretch-blow molding of PET bottles with parametric studies. *Polymer Engineering & Science*, *44*(7), 1379-1390.

Yeom, C. K., & Lee, K. H. (1996). Pervaporation separation of water-acetic acid mixtures through poly (vinyl alcohol) membranes crosslinked with glutaraldehyde. *Journal of Membrane Science*, *109*(2), 257-265.

Yoo, B. M., Shin, H. J., Yoon, H. W., & Park, H. B. (2014). Graphene and graphene oxide and their uses in barrier polymers. *Journal of Applied Polymer Science*, *131*(1).

Zeman, S., & Kubík, L. (2007). Permeability of polymeric packaging materials. *Technical Sciences/University of Warmia and Mazury in Olsztyn*, (10), 26-34.

Zhang, J., Yang, H., Shen, G., Cheng, P., Zhang, J., & Guo, S. (2010). Reduction of graphene oxide via L-ascorbic acid. *Chemical Communications*, *46*(7), 1112-1114.

Acknowledgments